Acta Geodyn. Geomater., Vol. 19, No. 4 (208), 319–341, 2022
DOI: 10.13168/AGG.2022.0016

journal homepage: https://www.irsm.cas.cz/acta

ORIGINAL PAPER

GEOTECHNICAL PERFORMANCE OF COMBINED STONE COLUMNS AND PILES CAPPED WITH REINFORCED CONCRETE RAFT FOUNDATION IN SOFT CLAY SOIL

Danish AHMED [1,2], Siti Noor Linda bt TAIB [1], Tahar AYADAT [2] * and Alsidqi HASAN [1]

[1] *Faculty of Engineering, Universiti Malaysia, Sarawak, Malaysia*
[2] *Civil Engineering Department, Prince Mohammad bin Fahd University, Saudi Arabia*

**Corresponding author's e-mail:* tayadat@pmu.edu.sa

ARTICLE INFO

Article history:
Received 8 November 2022
Accepted 19 December 2022
Available online 31 December 2022

Keywords:
Stone columns
Piles
Raft foundation
Combined
Soft soils

ABSTRACT

Stone columns consist of granular material compacted in long cylindrical holes. They are used for improving the strength and consolidation characteristics of compressible soils. However, they are still less effective at supporting heavy loads, since they still cannot transfer applied stresses to deeper layers of soil. The main objective of this numerical study was to investigate the geotechnical performance of a combined foundation system composed of stone columns and piles grouped together under a rigid raft foundation in compressible soil. The failure mechanism of this hybrid foundation system was examined, and configurations optimizing the performance of the combined foundation system were explored. An analytical model was developed for predicting the ultimate carrying capacity of the combined system in compressible soils. It was deduced that combining stone columns and piles in one foundation system improved considerably the system's carrying capacity. Moreover, the uppermost improvement was observed when the piles were installed on the periphery or edge of the raft foundation, while stones columns were placed at the center area of the raft. The failure of the combined foundation system started from the center of the raft and noticeably extended to its edges. Due to the presence of stone columns in the combined foundation system, the piles did not interact. The areas affected or influenced by the soil–pile interaction also did not overlap.

1. INTRODUCTION

Many countries have over recent decades seen a significant expansion in the number of new cities being built outside of their traditional inhibited zones. For them, geotechnical engineers have had to deal with completely new and problematic types of soil, including peats and soils that are collapsible, swelling, liquefiable, or soft (up to very soft). These soils can usually be found in lowland areas, such as in floodplains, streams, and lakes. It is now possible to classify, test, and construct on weakly compressible soils.

The most common type of troublesome soil is compressible soil, its main characteristics being high compressibility, low undrained shear strength (c_u less than 25 kPa), and low permeability. For this type of soil, construction problems generally include excessive compression under heavily loaded foundations, insufficient bearing capacity, differential settlement, and instability while excavating and forming embankments. It can be difficult for foundations to be designed in such soil. This problem is often overcome by using ground improvement techniques including pre-compression, sand drains, stone columns, and sand compaction piles, in addition to stabilization through mixtures, soil reinforcement, and pile foundations. In recent decades, several studies have been carried out on foundation improvement techniques, including piling, raft on piles, preloading compaction, soil reinforcement, and stone columns, to overcome and minimize the adverse effects of such soil conditions (e.g., Ali et al., 2010; Ayadat and Hanna, 2005; Elias et al., 2006; Han, 2015; Hussain, 2006; Jenck et al., 2005; McCabe et al., 2007; Mehrannia et al., 2018; Michael and Kirsch, 2004; Mishra, 2016; Singh and Kumar, 2019; Van, 1989).

Stone columns and pile foundations are the most common foundation systems currently used in soft and compressible soils. The implementation of stone columns involves adding vertical columns of stone into the ground to a sufficient depth below the surface to improve or provide reinforcement of the weak ground. In contrast, piles are structural members that are made mainly of steel or concrete that penetrate through weak soil layers to the stiff soil or bed rock. Many researchers have investigated the performance of stone columns under raft, concluding that increases in raft thickness, the diameter of stone columns, and the angle of shearing resistance of stone and decreased spacing in the stone columns can improve settlement and bearing capacity significantly. They also deduced that the length of stone columns has a slight effect on

Cite this article as: Ahmed D, bt Taib SNL, Ayadat T, Hasan A: Geotechnical performance of combined stone columns and piles capped with reinforced concrete raft foundation in soft clay soil. Acta Geodyn. Geomater., 19, No. 4 (208), 319–341, 2022. DOI: 10.13168/AGG.2022.0016

the performance of their foundation systems (e.g., Das and Deb, 2014; Ghazavi and Ashraf, 2013; Nazari and Ghazavi, 2014; Naseer et al., 2019; Nehab et al., 2017; Remadna et al., 2020; Sexton et al., 2014). Similarly, many researchers have studied piled raft foundation systems. It has been reported that by increasing the pile length, pile diameter, aspect ratio, number of piles, and raft foundation thickness, the overall performance of piled raft foundations improves considerably (e.g., El-Garhy et al., 2013; Lin and Feng, 2006; Mali and Sing, 2020; Sinha and Hanna, 2017; Vu et al., 2014; Xie and Chi, 2020).

As mentioned earlier, stone columns, which consist of granular material compacted in long cylindrical holes, are used to improve the strength and consolidation characteristics of compressible soil. Unlike pile foundations, they make very efficient use of the soil near the surface. Although they are ideal for light loads, they are less effective at supporting heavy ones because they cannot transfer the applied stresses to deeper layers of soil. For heavy structures, the strategy of deep foundations (piles) is very effective, because piles penetrate through the weak soil deposits to the stiff soil or bed rock to support the structure's weight. However, foundations with piles are more expensive than methods using stone columns and quite often have an economic impact on construction projects. The stone columns or groups of piles are typically capped by a reinforced concrete block known as a pile cap, which is responsible for making the piles work as a unit.

There have been very few works reported in the literature on the use of stone columns and pile foundations together as a composite foundation system under raft foundations in compressible soils. Manojit et al. (2017) investigated the performance of stone columns combined with piles under rigid raft (i.e., a combined foundation system) in soft soils. They found that the change in length, spacing, angle of shearing resistance of stone, area replacement ratio, diameter of stone columns/piles, and thickness of raft can change the percentage of shared load on the stone columns and piles. In addition, they stated that a detailed parametric study would be required for the optimization of foundation configurations and for designing an economical foundation system composed of stone columns and piles under rigid raft in soft soils.

The main objective of this research is to investigate the geotechnical performance of a combined foundation system composed of stone columns and piles grouped together under a rigid raft foundation in a compressible soil. In this study, the failure mechanism of the combined foundation system under uniform loading is examined**.** Furthermore, a parametric study is conducted to determine the configurations or the combinations of stone columns and piles that will enhance the geotechnical performance of the combined foundation system. In this respect, a wide range of configurations is analyzed, and the most relevant ones, from a carrying capacity point of view, are considered upgrade and optimal. Additionally, an analytical model to predict the carrying capacity of the combined foundation system capped with a rigid raft foundation in compressible soils is developed and validated.

2. METHODOLOGY

It is believed that combined foundation systems (i.e., stone columns combined with piles under rigid raft) are the most attractive solution for optimizing the cost and performance of foundations in soft soils. To investigate the geotechnical performance of these, numerical modeling and analysis was performed using Plaxis 3D, a three-dimensional finite element software program.

The geometry of the three-dimensional model was selected based on trials to avoid horizontal and vertical stress confinement. The overall size of the complete 3D model was 100 m×100 m×40 m. For the boundary condition of the 3D model, there was considered to be a fixed support at the bottom, and roller supports were assumed to be on the vertical boundaries, as shown in Figure 1. A uniform distributed load of 20 m×20 m rigid raft was applied on the surface (Fig. 1).

Mesh size plays an important role in any finite element modeling. Using fine mesh can capture results very close to the real behavior of the model, but it can consume more time for analysis, and vice versa. In the present study, 10-noded tetrahedral elements were used to create a 3D model for all soil elements and stone columns. Medium mesh size was used globally for the model, and it was refined to fine and very fine near the region where critical stresses and displacements were expected (Figs. 2 and 3).

Selecting material properties and model type in any form of numerical modeling is very important for a definite simulation. Plaxis 3D provides model types for all kinds of element involved in geotechnical investigations. In the present study, the Mohr–Coulomb model was considered for modeling all soil elements. The different soil layers (i.e., the soft clay and the thick sand layer situated beneath the soft clay) were modeled using the elastic–perfectly plastic model. The Mohr–coulomb model works with five very common parameters, namely Young's modulus (E), Poisson's ratio (v), cohesion (c), the friction angle (φ), and the dilatancy angle (ψ). Stone columns were also modeled using the elastic–perfectly plastic Mohr–Coulomb failure criteria. The granular stone column material was considered in drained conditions. The concrete raft was modeled using the linear elastic model, which is based on the Hooke's law. This model mainly requires two parameters, namely Young's modulus and Poisson's ratio, and is suitable for modeling stiff structural elements. The piles were modeled using the embedded pile option, which works as a beam element model. Embedded piles can be modeled in the soil at any arbitrary direction that connects and interacts with soil elements using special skin resistance and foot resistance interface elements. The parameters required for the embedded pile model

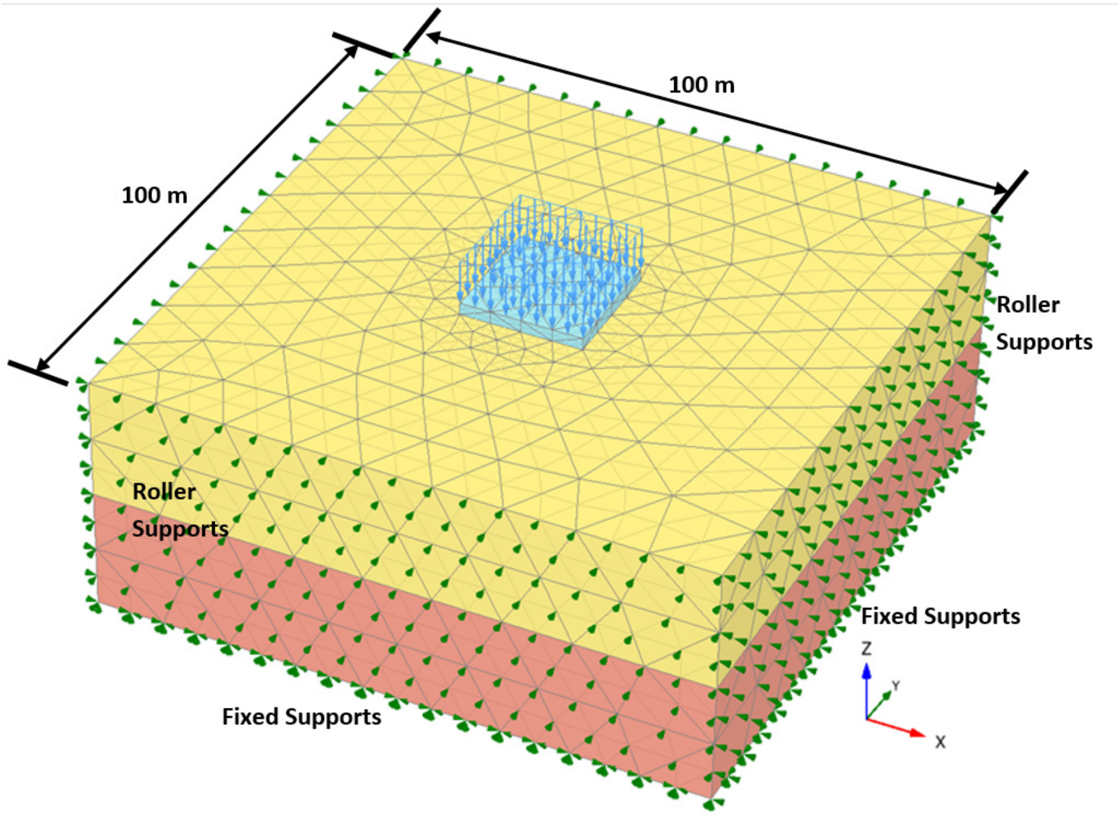

Fig. 1 Plaxis 3D model with boundary conditions.

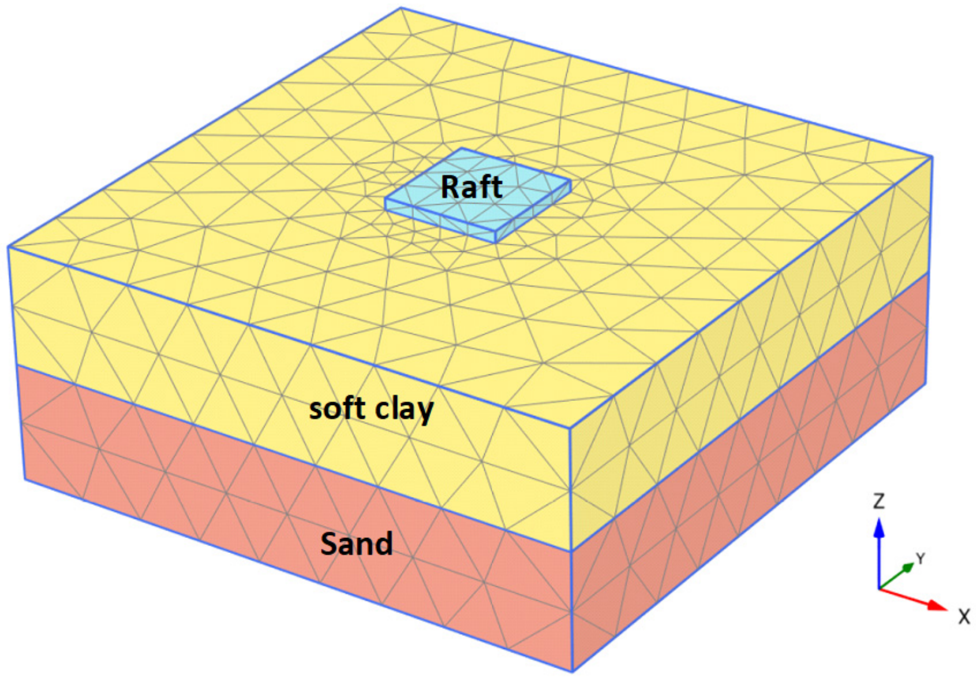

Fig. 2 Model's overall meshing.

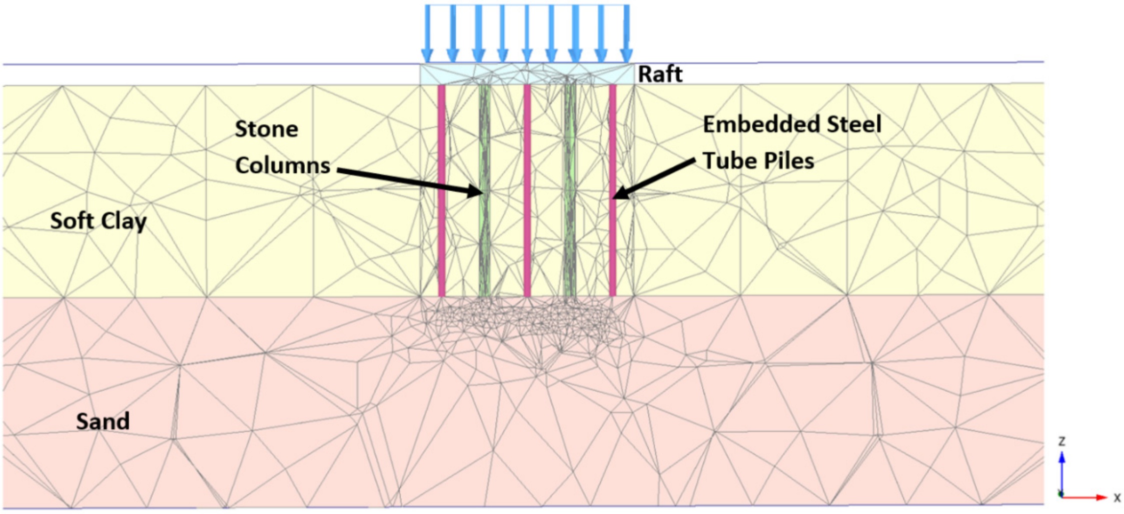

Fig. 3 Model's refined meshing.

Table 1 Material properties for the stone column, piles, and rigid raft.

Properties	Soft clay	Sand	Stone column	Pile	Raft
Unit weight, γ(kN/m^3)	17, 18	17.5, 19.5	19, 20	–	–
Young's modulus, E_s(MPa)	4, 6, 8	28	80	210×10^3	27.8×10^3
Poisson's ratio, νs	0.5	0.3	0.3	–	0.15
Angle of friction, φ (°)	0	42	42, 45, 48	–	–
Cohesion, c (kN/m^2)	25	0	0	–	–
Diameter (m)	–	–	1	0.4, 0.5, 0.6	–
Length (m)	–	–	20, 18, 16, 12	20	–

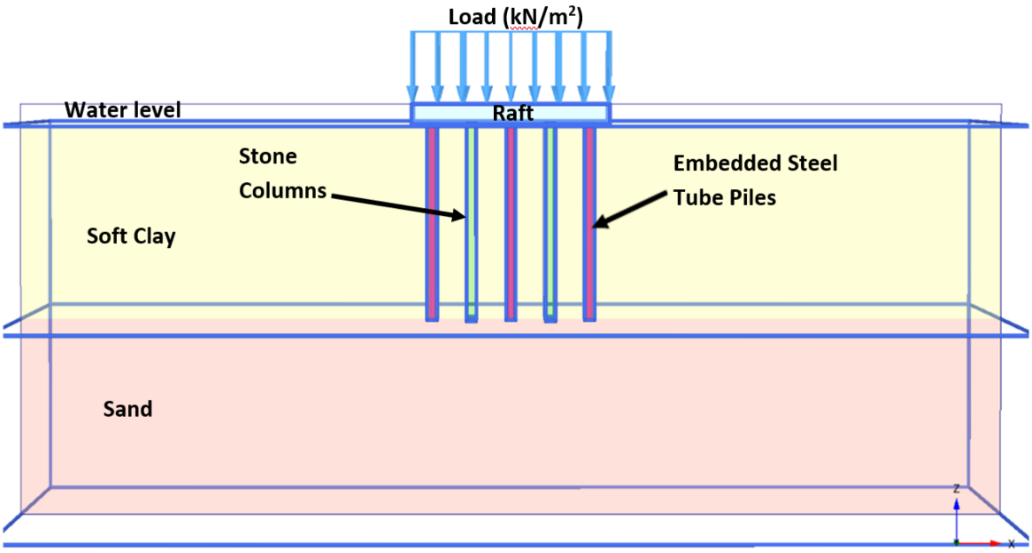

Fig. 4 Different components of the model (in 2D).

are the same as those required for the linear elastic beam elements. It is worthwhile to note that the Mohr–Coulomb elastic–perfectly plastic model was adopted in the present study because it is convenient for the limit equilibrium state, which is adopted when developing the analytical model. Furthermore, several numerical analyses reported in the literature that employed the Mohr–Coulomb model were in good agreement with the physical modeling or the experimental data (e.g., Etezad et al., 2015; Samangani and Naderi, 2022). The material properties of the different components of the foundation system (i.e., soft soil, stone columns, piles, and rigid raft) used in this investigation are summarized in Table 1. The different components of the studied model are illustrated in Figures 4 and 5.

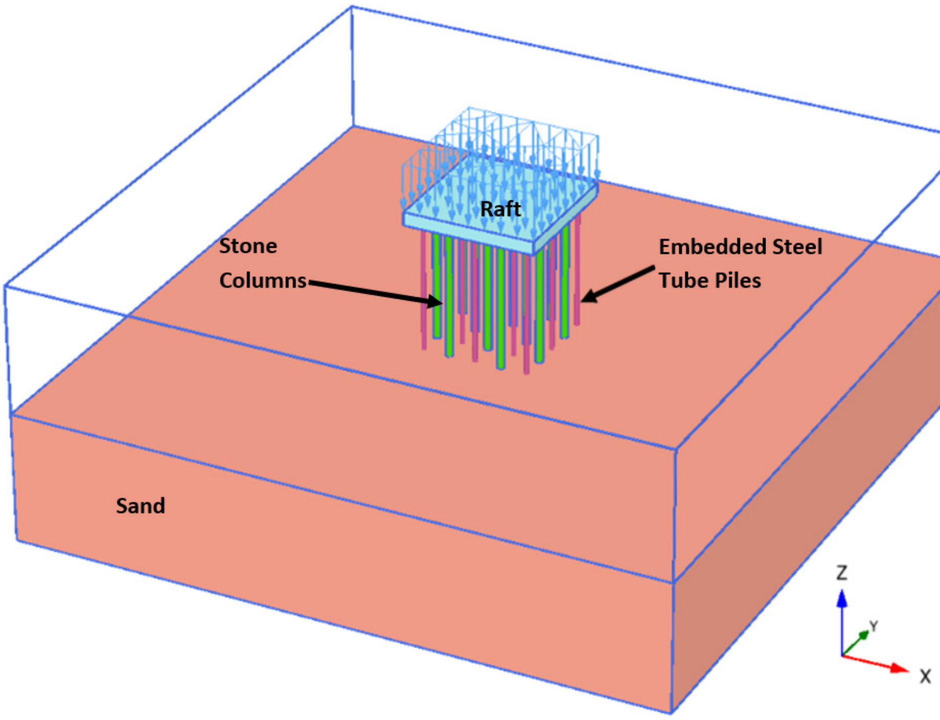

Fig. 5 Different components of the model (in 3D).

Table 2 Distribution of sets in each group.

Group No.	No. of piles	Distribution of sets in each group (Appendix A)
1	4	2, 8, 24, 25
2	5	10, 22, 29, 30
3	8	3, 9, 14, 26, 27
4	9	11, 18, 23, 31, 32
5	12	15, 16, 28
6	13	19, 20, 33
7	16	4, 17
8	17	12, 21
9	20	5
10	21	13
11	24	6

In this investigation, a total of 25 stone columns and piles were arranged in 34 different configurations (or sets), as shown in Appendix A. These configuration (or set) were categorized into 11 groups based on the number of piles in each group, as indicated in Table 2. Furthermore, for the parametric study, every set was considered in 20 combinations, depending on the geometry of the stone columns and piles and the material properties of the stone columns and the soft soil, as shown in Table 3. It is worthy of mentioning that the data regrouped in Table 1 represent the parameters of the range of soil sand the dimensions of stone columns and piles encountered in practice. The data combinations of Table 3 were extracted from the input of Table 1 for the purpose of the parametric study and to imitate some field conditions. The configurations of the column–piles arrangement presented in Table 2 were adopted with respect to the number of piles and their emplacement in each configuration. The number and positioning of the piles was varied to cover a wide range of conceivable combinations.

As discussed earlier, very few studies have investigated the performance of combined foundation system in soft soils. For this reason, the numerical model developed in this investigation was validated for two cases separately, namely soft soil reinforced with stone columns alone (case #1) and soft soil strengthened with piles (case #2). For case #1, the numerical results obtained in this study for stone columns alone were validated against the experimental results reported by Ghazavi and Afshar (2013). However, for case #2, the results of the present numerical analysis for a piled raft foundation were

Table 3 Data considered in each combination.

Combination no.	Stone column length (m)	Stone column diameter (m)	Pile length (m)	Pile diameter (m)	Young's modulus of soft clay (MPa)	Angle of friction for stone columns φ (º)
1	20	1	20	0.6	4	45
2	20	1	20	0.5	4	45
3	20	1	20	0.4	4	45
4	18	1	20	0.6	4	45
5	18	1	20	0.5	4	45
6	18	1	20	0.4	4	45
7	16	1	20	0.6	4	45
8	16	1	20	0.5	4	45
9	16	1	20	0.4	4	45
10	12	1	20	0.6	4	45
11	12	1	20	0.5	4	45
12	12	1	20	0.4	4	45
13	20	1	20	0.5	8	45
14	20	1	20	0.5	6	45
15	16	1	20	0.5	8	45
16	16	1	20	0.5	6	45
17	20	1	20	0.5	4	48
18	20	1	20	0.5	4	42
19	16	1	20	0.5	4	48
20	16	1	20	0.5	4	42

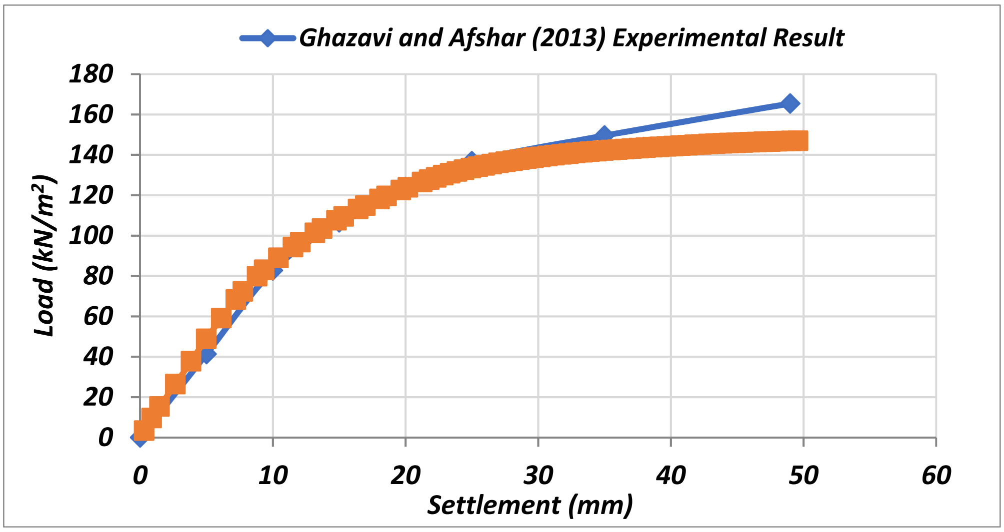

Fig. 6 Model validation for stone columns alone under raft.

endorsed against the numerical results of Sinha and Hanna (2017). Figures 6 and 7 show the results of these comparisons for case #1 and case #2, respectively. A good agreement was noted between the results obtained from the present numerical model and the experimental and numerical data reported in the literature. The confirmation of the validity of the models for stone columns alone and for piled raft suggests that it is reasonable to believe that the present model should have validity when applied to a combined foundation system.

3. RESULTS AND DISCUSSION

The effect of the model's geometry and the materials' properties on the performance of the combined foundation system in soft soil was studied, and the failure mechanism of this foundation system under uniform loading was examined. As mentioned earlier, based on the parameters studied, 20 combinations were considered for each of the 34 configurations presented in Appendix A. Overall, 680 combinations were investigated in the present parametric study, the results of which are discussed in the following sections. It is worthy of note that, due to space limitation, only typical results are presented.

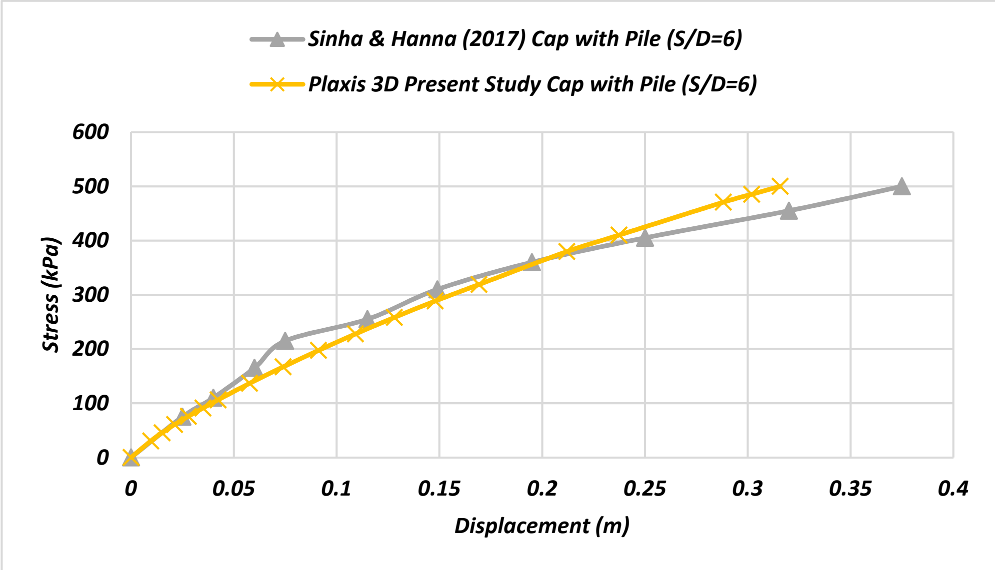

Fig. 7 Model validation for piled raft.

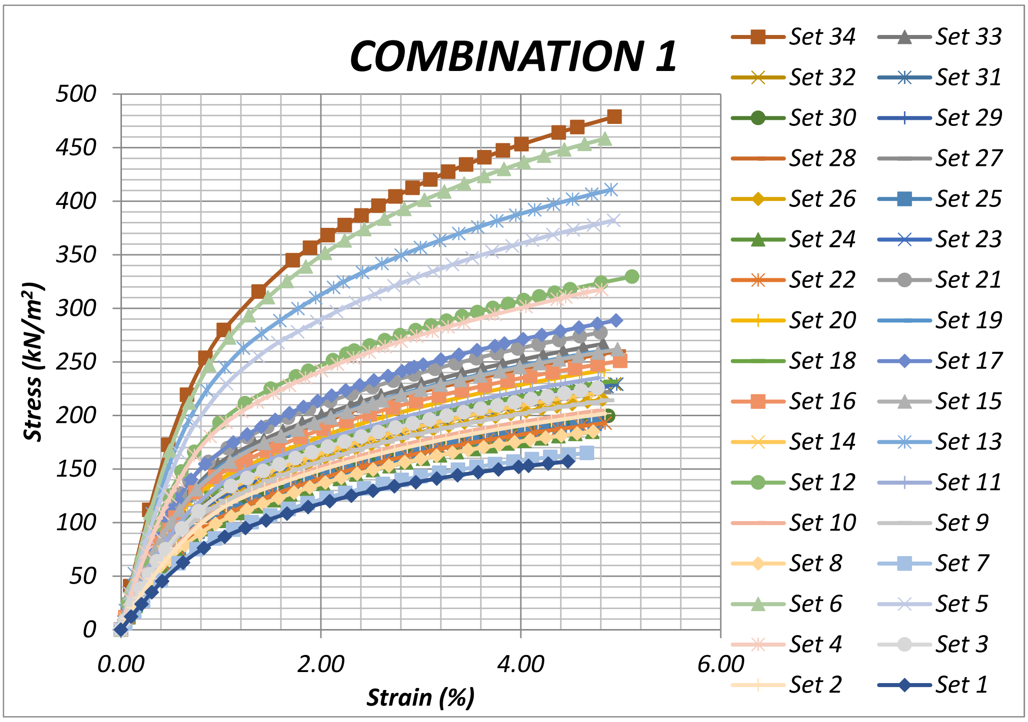

Fig. 8 Stress–strain curves for combination 1 of the combined foundation system.

Nevertheless, the results of the 680 combinations are described in Ahmed (2023). Furthermore, for the purpose of comparison, the term improvement factor (*IF*) has been introduced. It is defined as the ratio between the ultimate carrying capacity of the combined foundation system to that of raft foundation with stone columns alone.

3.1. EFFECT OF CONFIGURATION ON THE PERFORMANCE OF THE COMBINED FOUNDATION SYSTEM

To study the configuration effect on the performance of the combined foundation system, stress–strain diagrams of the 680 combinations were established. The typical stress–strain diagrams for combination 1 are presented in Figure 8. The curves represent the variation of the stresses applied on the raft foundation against the corresponding strains. In the numerical simulations, the stress was applied progressively by increments to the top of the rigid raft foundation, and the corresponding displacement of the raft was recorded. The strain was then computed as a ratio of the displacement and the initial length of the piles. The results indicated that increases in the number of piles in the different configurations (or sets) increased the overall capacity of the combined foundation system (Fig. 8). Also, a significant difference of carrying capacity was noted between set

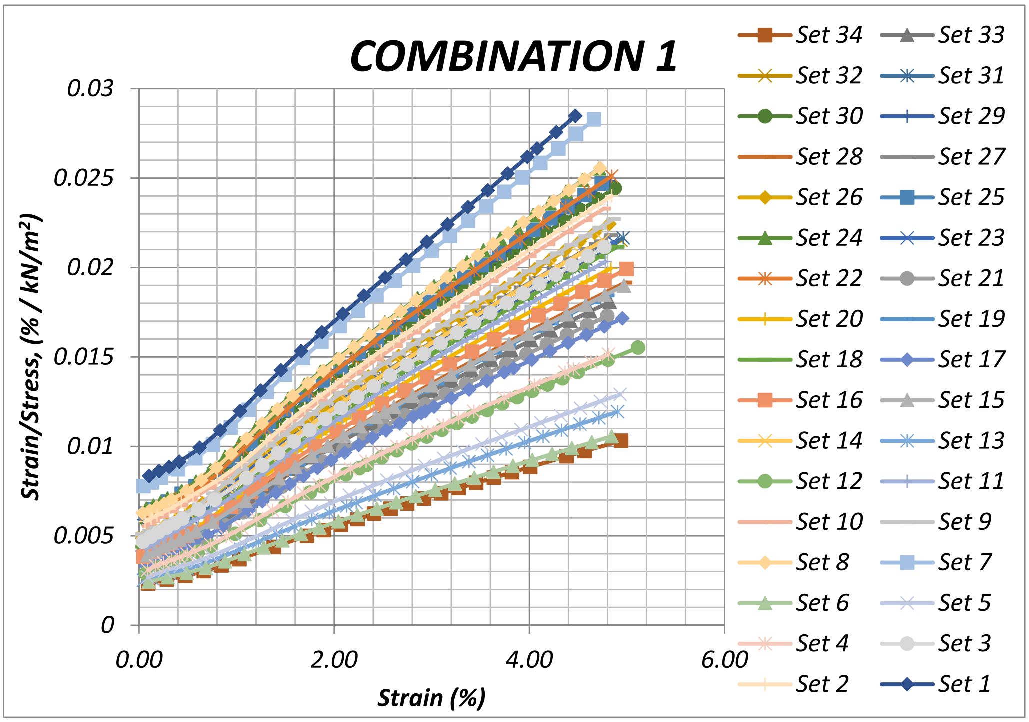

Fig. 9 Variation of the strain–stress ratio with strain for combination 1 of the combined foundation system.

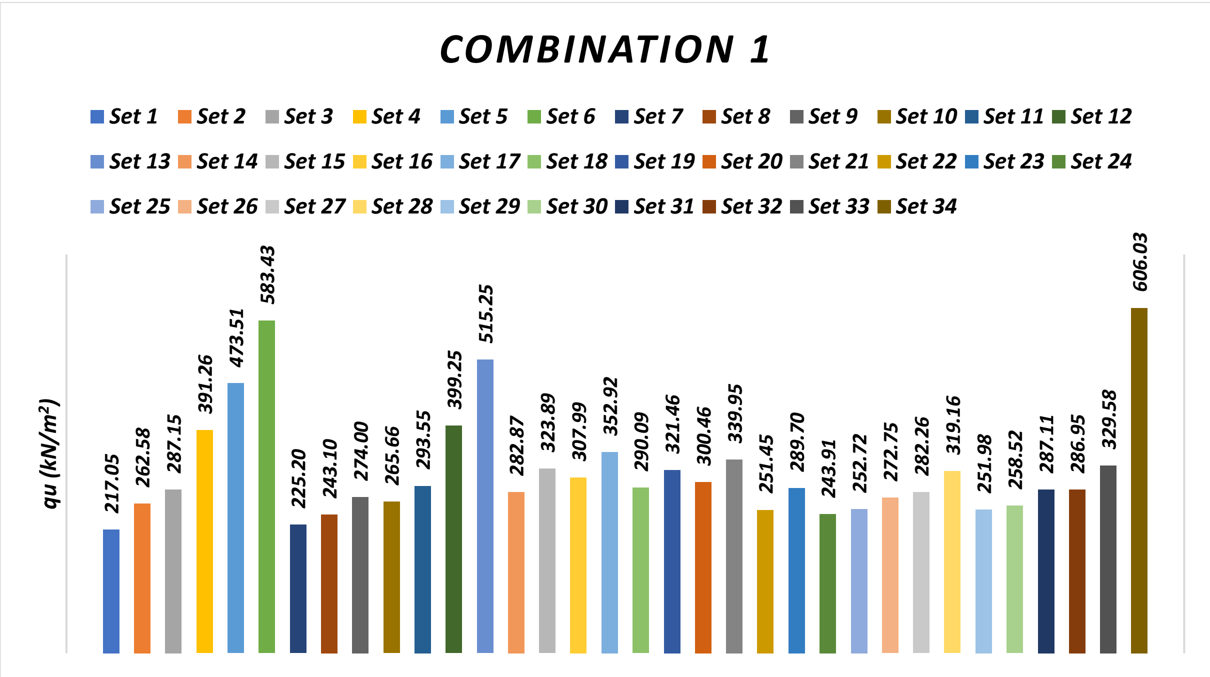

Fig. 10 Ultimate carrying capacities of combination 1 of the combined foundation system.

1 (stone columns with raft foundation) and set 34 (piled raft foundation). However, the stress–strain curves of the different sets did not show any clear sign of failure. Therefore, Chin's (1970) stability method was used to predict the ultimate carrying capacity of the different combined foundation systems. In this method, the values of the ratio of the strain to the stress plotted against the strain resulted on a straight line, and the inverse slope of this line was the ultimate carrying capacity (Fig. 9).

The different values of the ultimate carrying capacity determined by Chin's method for all sets are presented as column charts. A typical column chart for combination 1 is presented in Figure 10 and confirms that by increasing the number of piles in the sets, the ultimate carrying capacity of the combined foundation systems increased. It is worthwhile to note that Sets 6, 13, and 34 showed the highest values for ultimate carrying capacity, since they had the highest number of piles in the arrangement.

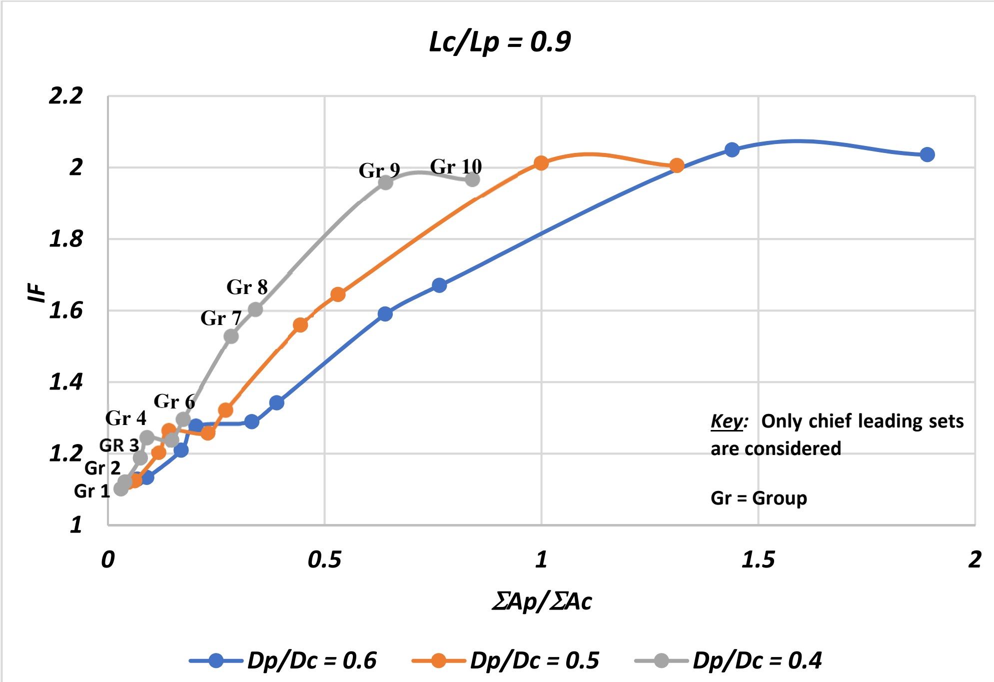

Fig. 11 Typical variation of IF versus $\Sigma A_p/\Sigma A_c$ and D_p/D_c for $L_c/L_p = 0.9$.

3.2. EFFECT OF THE DIAMETER OF STONE COLUMN AND PILES ON THE PERFORMANCE OF THE COMBINED FOUNDATION SYSTEM

It is believed that the diameters of stone columns and piles are among the governing parameters influencing the performance of the combined foundation system. To investigate the effect of these measurements on the performance of the combined foundation system, three ratios of piles' diameter to that of stone columns (D_p/D_c) were considered; in this case, D_p/D_c= 0.6, 0.5, and 0.4. Figure 11 shows a typical variation of the *IF* versus the ratio of the sum of the piles' area to the sum of the stone columns' area($\Sigma A_p/\Sigma A_c$) for different ratios of D_p/D_c and for the piles' length to the stone columns' length (L_c/L_p) = 0.9. Each point of the different curves shown in Figure 11 was identified by its corresponding group number. Only chief sets were considered in the construction of these individual curves. It is clear from this figure that by increasing the diameter ratio D_p/D_c and the area ratio $\Sigma A_p/\Sigma A_c$, the *IF* increased up to 2. For a given ratio $\Sigma A_p/\Sigma A_c$, the *IF* was higher when the ratio D_p/D_c was equal to 0.4. This is because to maintain a constant ratio $\Sigma A_p/\Sigma A_c$, the number of piles in the foundation system is increased when the diameter of piles is decreased. Moreover, it can be deduced from this figure that the overall performance of the combined foundation system was improved considerably.

3.3. EFFECT OF STONE COLUMN AND PILE LENGTH ON THE PERFORMANCE OF THE COMBINED FOUNDATION SYSTEM

To study the effect of stone columns' and piles' lengths on the performance of the combined foundation system, four different length ratios of stone columns to piles (L_c/L_p) were considered; in this case, L_c/L_p= 1, 0.9, 0.8, and 0.6. Figure 12 shows a typical variation of the improvement factor versus the ratio ($\Sigma A_p/\Sigma A_c$) for different ratios L_c/L_p and for the case of D_p/D_c = 0.5. Likewise, with a decrease in the length ratio of stone columns to piles (L_c/L_p), the improvement factor increased. For a given ratio $\Sigma A_p/\Sigma A_c$, the improvement factor was higher when the ratio L_c/L_p= 0.6, and equal to lower for L_c/L_p= 0.8, 0.9, or 1. This can be attributed to the fact that, beyond the critical length, reported to be equal to six times D_c (Ayadat, 2022), the columns do not contribute extra benefit in terms of enhanced ultimate load, but they help to reduce settlement by penetrating the firm stratum. Nevertheless, the overall performance of the combined foundation system was generally more than double.

3.4. EFFECT OF THE ANGLE OF SHEARING RESISTANCE OF STONE COLUMNS ON THE PERFORMANCE OF THE COMBINED FOUNDATION SYSTEM

The influence of the angle of shearing resistance of stone column materials (φ_c) on the performance of the combined foundation system was also considered in the present parametric study. Three values of the angle of shearing resistance of stone column materials were selected, namely φ_c= 42°, 45°, and 48°. A typical variation of the improvement factor (*IF*) with the angle of shearing resistance (φ_c) and the area ratio ($\Sigma A_p/\Sigma A_c$) is illustrated in Figure 13. The curves shown in this figure represent the results obtained for the length ratio L_c/L_p = 1. As expected, for a given area ratio

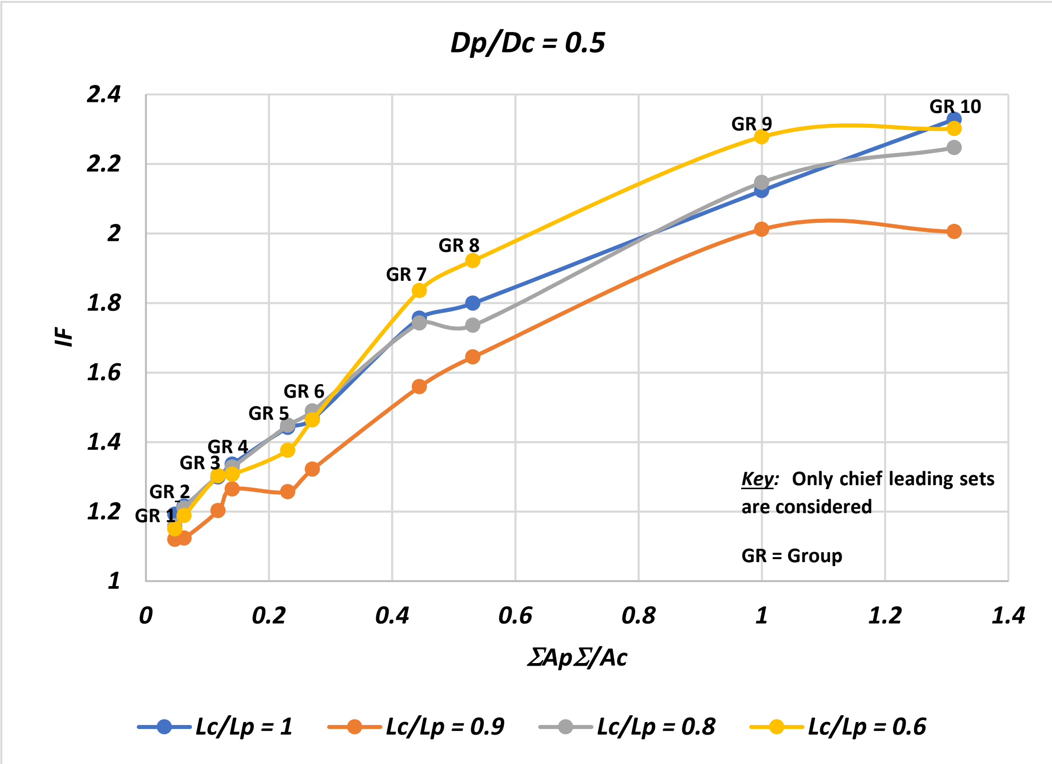

Fig. 12 Typical variation of IF versus $\Sigma A_p/\Sigma A_c$ and L_c/L_p for $D_p/D_c = 0.5$.

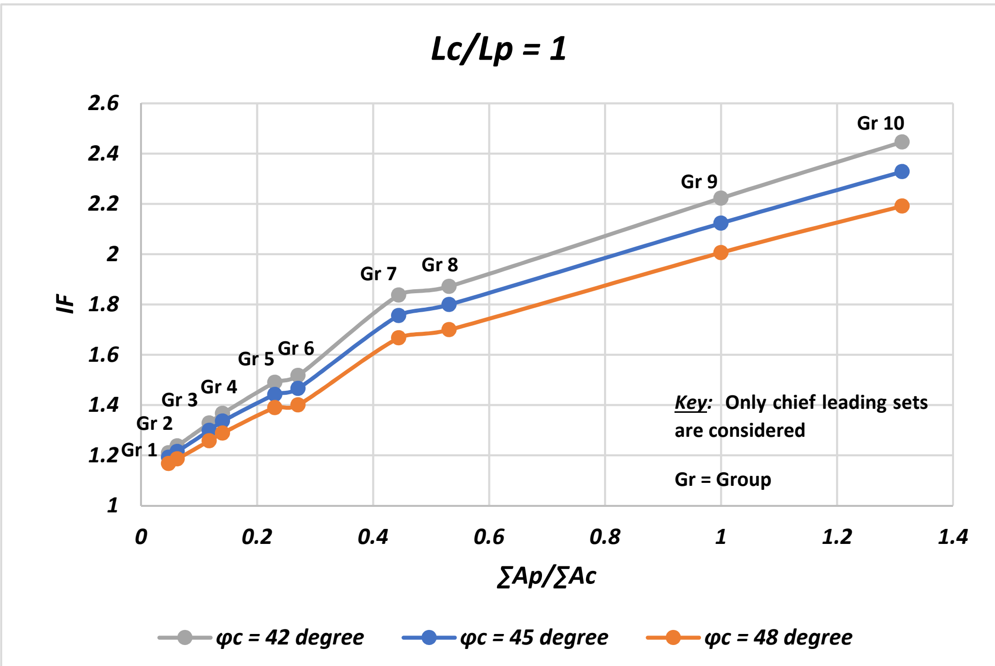

Fig. 13 Typical variation of IF versus $\Sigma A_p/\Sigma A_c$ and φ_c for $L_c/L_p = 1$.

($\Sigma A_p/\Sigma A_c$), the carrying capacity of raft on the combined stone columns and piles or raft on stone columns alone increased by increasing the angle of shearing resistance of the column material. However, the ratio between the carrying capacity of the combined foundation system and that of raft on stone columns (i.e., the improvement factor *IF*) increased with a decrease in the angle of shearing resistance of the stone column material. It was observed that when the angle of shearing resistance of the stone column decreased, the carrying capacity of raft on the stone columns alone decreased more swiftly than the carrying capacity of raft on the combined stone columns and piles. This can be explained by the existence of a higher number of columns in the first system.

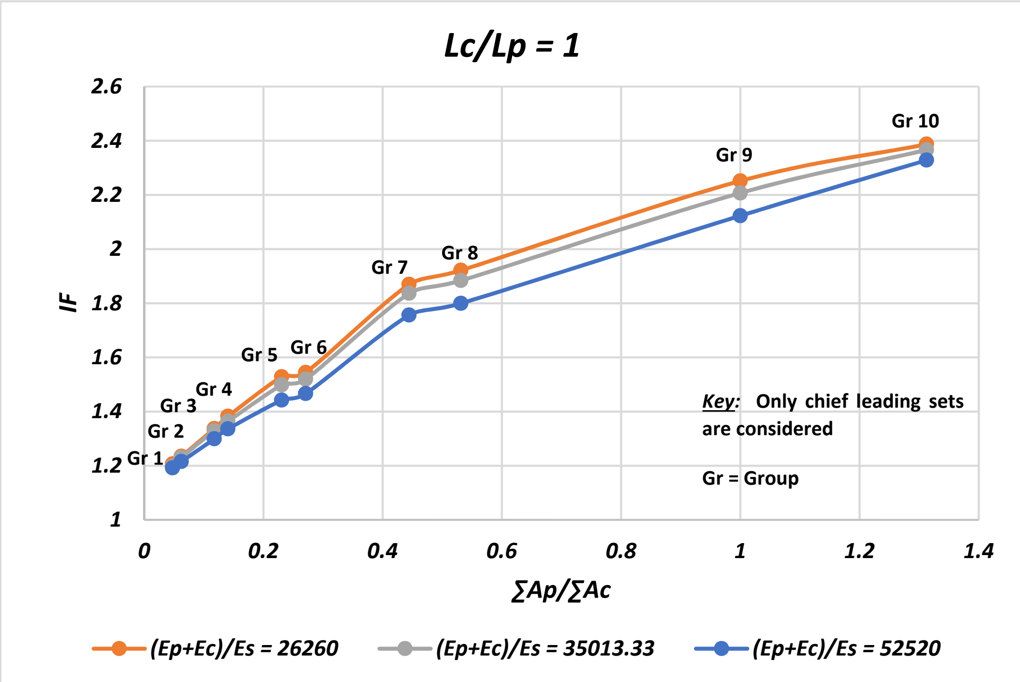

Fig. 14 Typical variation of IF versus $\Sigma A_p/\Sigma A_c$ and $(E_p+E_c)/E_s$ for $L_c/L_p = 1$.

3.5. EFFECT OF THE MODULUS OF ELASTICITY OF SOFT SOIL ON THE PERFORMANCE OF THE COMBINED FOUNDATION SYSTEM

The influence of the modulus of soft clay (E_s) on the performance of the combined foundation system was also examined. For this purpose, three values of the modulus of elasticity of soft clay were considered, namely E_s = 4, 6, and 8 MPa. Figure 14 shows a typical variation of the *IF* versus the rigidity ratio $(E_p+E_c)/E_s$ and the area ratio $(\Sigma A_p/\Sigma A_c)$ for the case of length ratio $L_c/L_p = 1$. The rigidity ratio $(E_p+E_c)/E_s$ is defined as the ratio between the sum of the modulus of elasticity of piles and stone columns and the modulus of elasticity of soft clay. It can be noted from this figure that the *IF* slightly increased with an increase in the modulus of elasticity of soft clay (i.e., with the decrease of the rigidity ratio $(E_p+E_c)/E_s$). Furthermore, the improvement factor was lower for piles with higher modulus of elasticity (higher rigidity). This can be explained by the fact that rigid piles penetrate more easily the layer of sand situated beneath the layer of soft soil. However, it is worth noting that this soil parameter (E_s) is commonly applied as a governing parameter for pile settlement analysis, rather than for carrying capacity (Ahmed et al., 2022).

3.6. CONFIGURATIONS ENHANCING THE PERFORMANCE OF THE COMBINED FOUNDATION SYSTEM

As mentioned earlier, 34 configurations (or sets) of combined stone columns and piles capped by rigid raft were considered. They were categorized into 11 groups based on the number of piles in each group. Additionally, each configuration was considered in 20 combinations depending on the geometry of the stone columns and the piles and the properties of the stone columns and the soft soil. A total of 680 finite element model simulations were tested. The improvement factor (*IF*) values for all 680 models were computed. Then the leading sets, with the highest improvement factor in each group for the 11 groups, were determined (Table 4). Typical results for the leading sets of group 1 are shown in Figure 15.

The 11leading sets presented in Table 4 were compared based on their *IF*, and sets 28, 33, 4, and 12 were selected as the chief leading sets. Sets 28 and 33 had a similar layout, as the piles in these sets were positioned at the center of the raft in the form of a plus sign (+), whereas in sets 4 and 12, the piles were positioned on the edges of the raft, as shown in appendix A. It is important to note that although sets 5, 13, and 16 had the highest improvement factor, they were discarded because the stone columns in these cases were almost entirely replaced with piles. This was out of the scope of the present investigation. In addition, sets 2, 10, 3, and 11 were not selected because they had lower improvement factor values. It is imperative to note that the chief leading sets (i.e., sets 28, 33, 4, and 12) showed performance superior to the raft foundation resting on the stone columns alone. It was deduced from the obtained values of the *IF* that the chief leading sets could increase the carrying capacity of the raft foundation by almost 60–100 %, compared with that of raft foundation resting on stone columns alone. Therefore, the arrangements of the stone columns and piles shown in sets 4, 12, 28, and 33 were the more appropriate or applicable in-situ disposition of the combined foundation system.

Eventually, to show the cost effectiveness of the chief leading sets when compared with a system composed solely of steel piles with comparable bearing capacity, the numerical model developed by

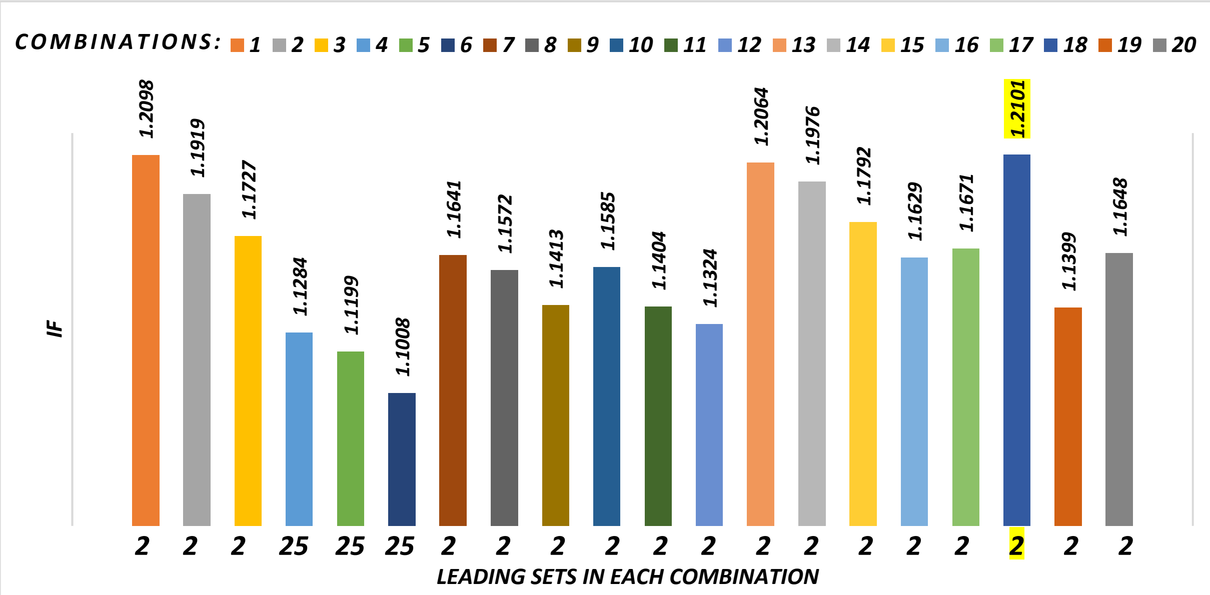

Fig. 15 The values of the IF for group.

Table 4 Leading set in each of the 11 groups.

Group no.	No. of piles in each group	Distribution of sets in each group	Leading set in each group Set	IF
1	4	2, 8, 24, 25	2	1.2101
2	5	10, 22, 29, 30	10	1.2498
3	8	3, 9, 14, 26, 27	3	1.3532
4	9	11, 18, 23, 31, 32	11	1.4044
5	12	15, 16, 28	**28***	**1.5284**
6	13	19, 20, 33	**33***	**1.5444**
7	16	4, 17	**4***	**1.8734**
8	17	12, 21	**12***	**1.9471**
9	20	5	5	2.2984
10	21	13	13	2.4461
11	24	6	6	2.8247

Note. *chief leading sets.

Ahmed et al. (2022) for piles in soft clayey soil was utilized. It was deduced that, for comparable carrying capacity, the cutback in the total area of the piles was reduced by about 40 % for the combined foundation system. Keeping in mind that stone columns are noticeably lower in price than piles, it is quite clear that the combined foundation system is more competitive than a system composed solely of steel piles.

3.7. *FAILURE MECHANISM OF THE COMBINED FOUNDATION IN SOFT SOIL*

The failure mechanism of the combined foundation system under uniform loading was examined. Based on the results obtained from the optimization study, only the failure mechanisms of the chief leading sets (i.e., sets 28, 33, 4, and 12) were studied. The failure mechanism of each set was examined in three different sections (the center, the edge, and the middle of the distance between the center and the edge of the set). The failure mechanisms of sets 4 and 28 are shown in Figures16 and 17. The general trend for the failure mechanism of the combined foundation system shows that the foundation failed by shear in the stone columns and soft soil and by bearing and shear failure of the piles' tip under the rigid raft. Moreover, it is clear from these figures that the failure of the combined foundation system started slightly from the center of the raft and noticeably extended to its edges. Moreover, due to the presence of stone columns in the combined foundation system, the piles did not interact. Also, as denoted by the strain regions displayed in Figures 16 and 17, the areas affected or influenced by the soil–pile interaction did not overlap. This observation contributes to the improvement of the geotechnical performance of the combined foundation system, since the carrying capacity of the piles is not reduced.

4. THEORETICAL DEVELOPMENT

The observed failure mechanism of the combined foundation system (Figs. 16 and 17) was used to develop an analytical model for predicting the system's ultimate carrying capacity. The analysis was

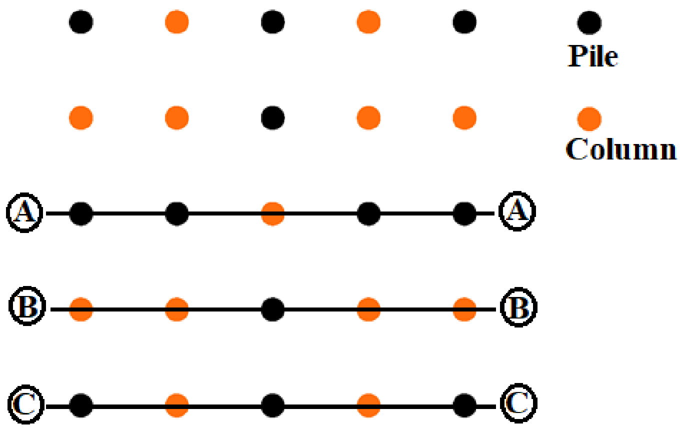

Fig. 16a Configuration #28.

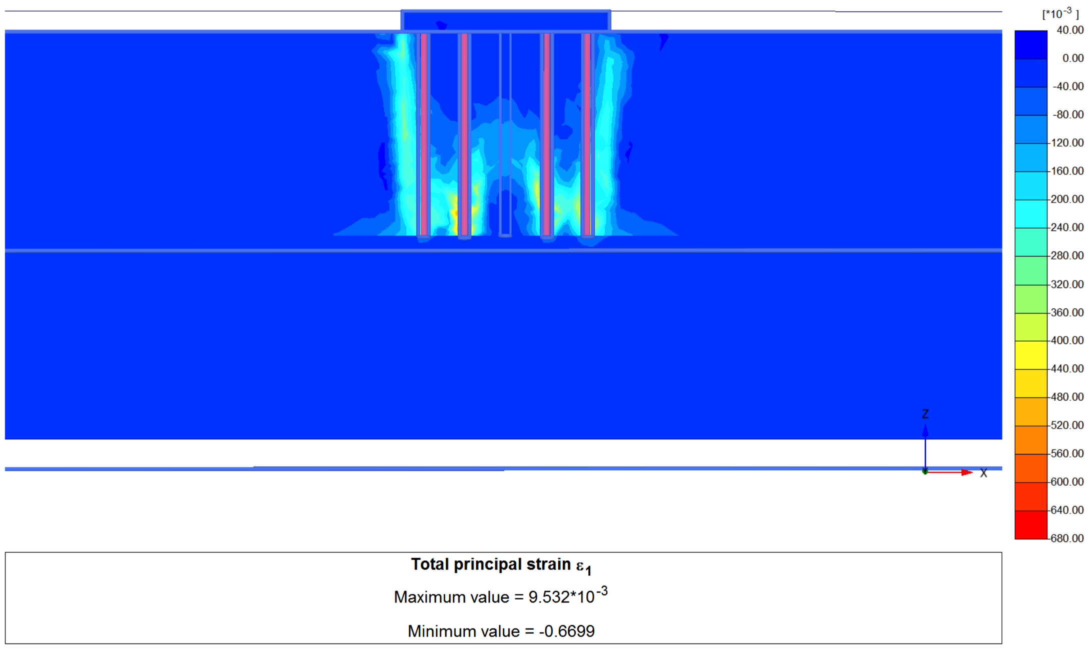

Fig. 16b Failure mechanism of the chief leading Set #28 at Section A-A.

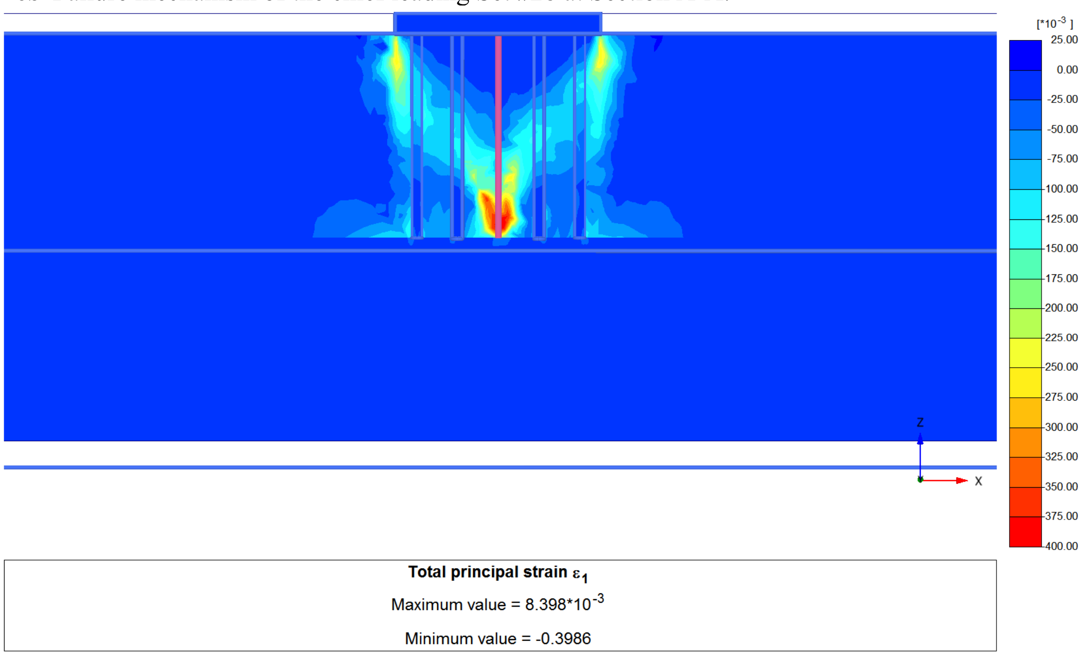

Fig. 16c Failure mechanism of the chief leading Set #28 at Section B-B.

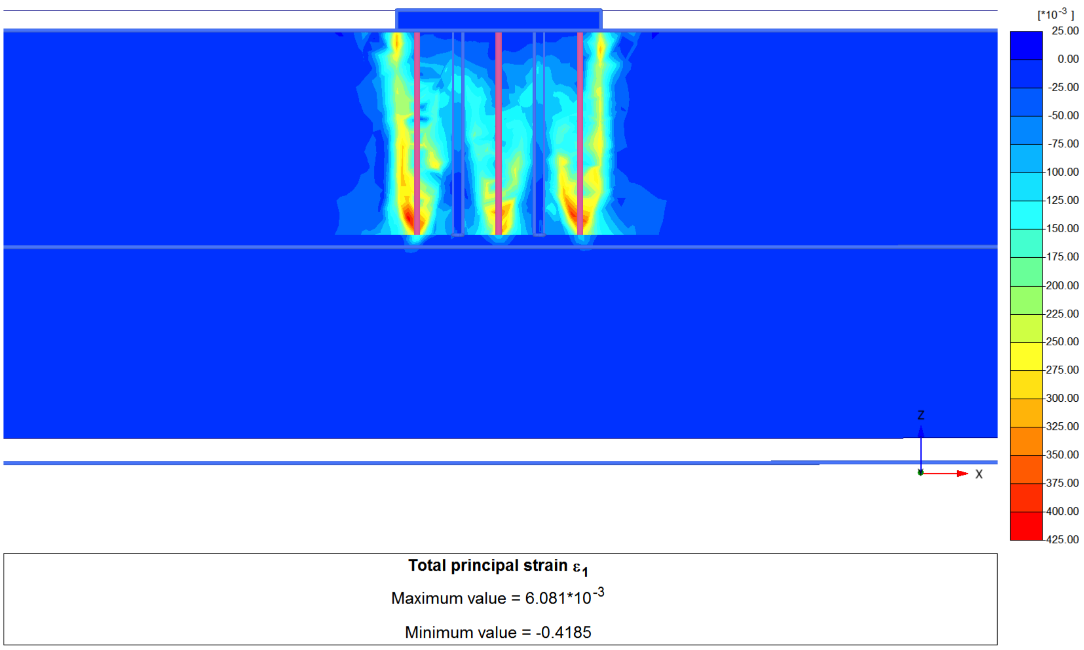

Fig. 16d Failure mechanism of the chief leading Set #28 at Section C-C.

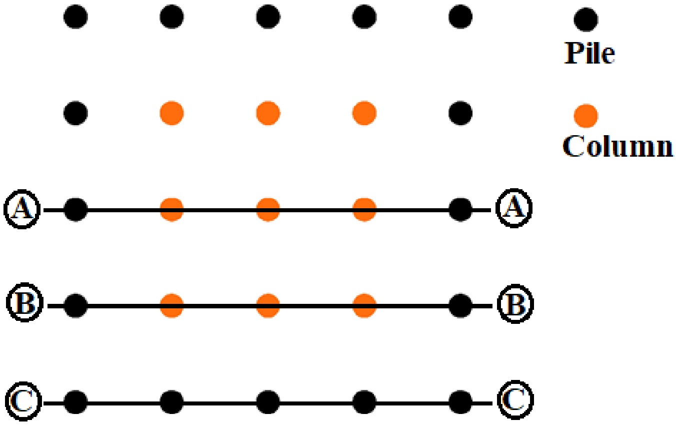

Fig. 17a Configuration #4

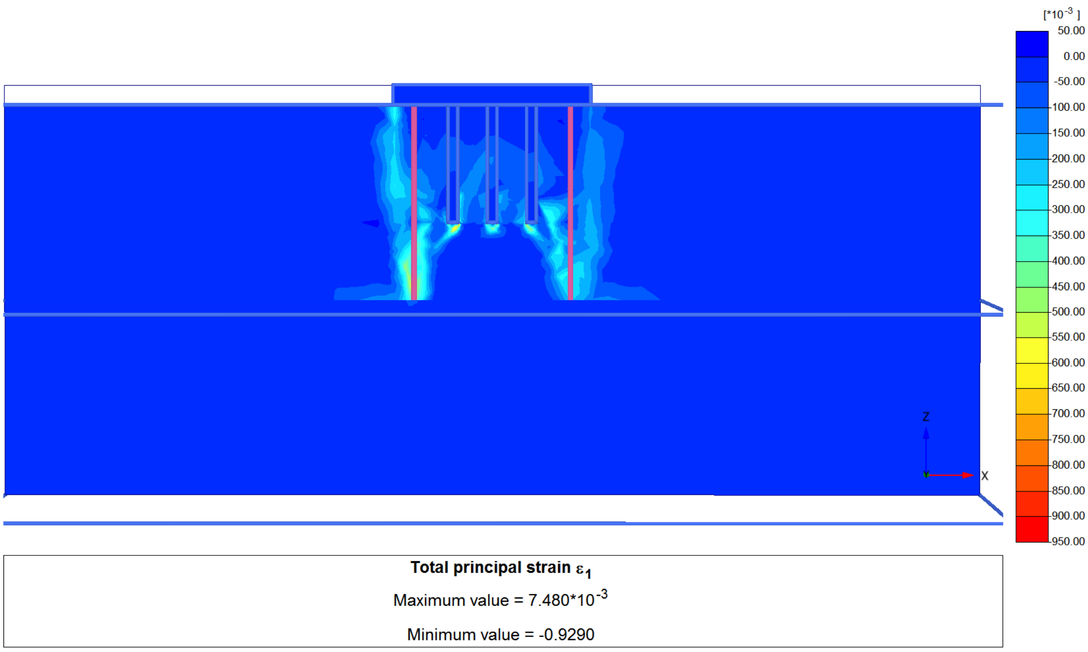

Fig. 17b Failure mechanism of the chief leading Set #4 at Section A-A.

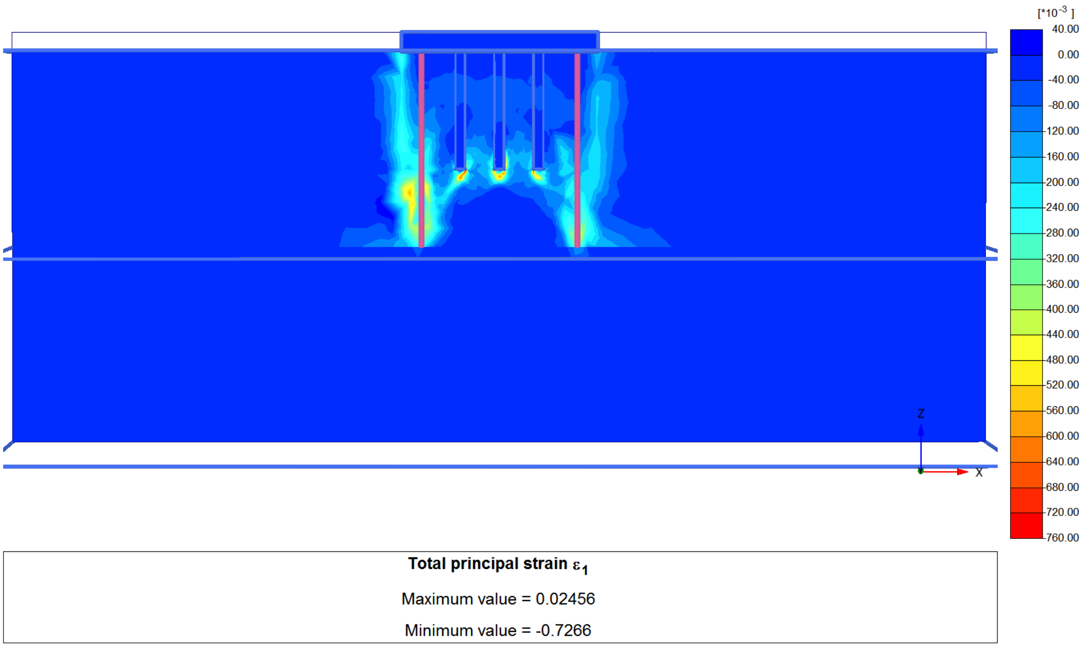

Fig. 17c Failure mechanism of the chief leading Set #4 at Section B-B.

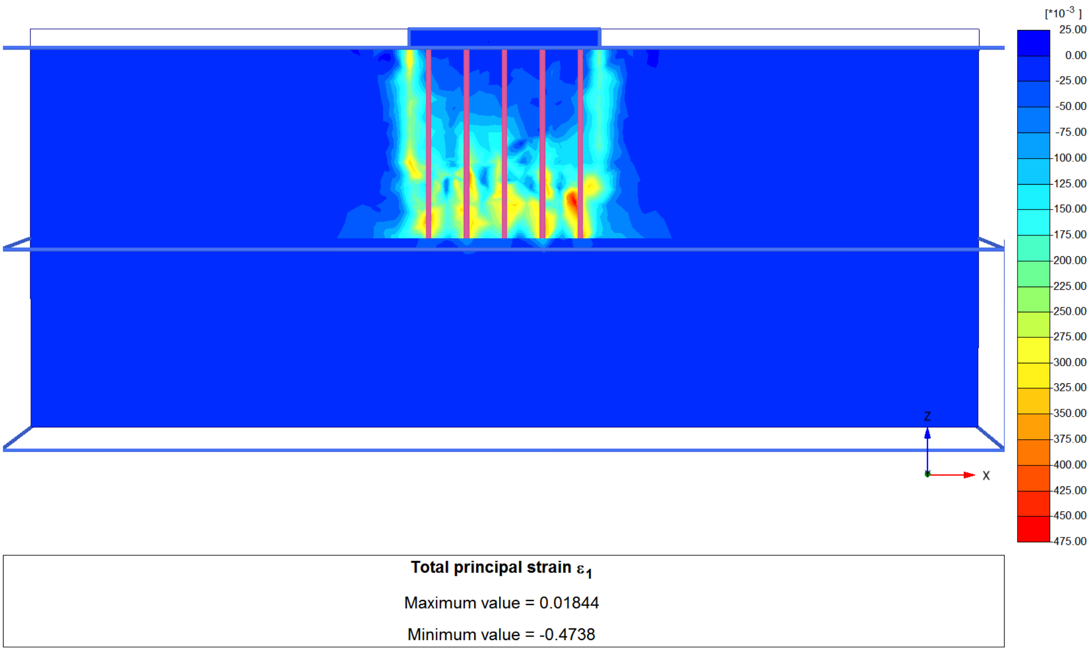

Fig. 17d Failure mechanism of the chief leading Set #4 at Section C-C.

based on the limit equilibrium method, the principal of homogeneous composite material (i.e., homogeneous soil composite made of the columns' material and soft clay), and the principal of superposition.

Using the principal of superposition, the ultimate carrying capacity of the combined foundation can be represented as follows:

$$Q_u = \alpha(Q_{u1} + n_1 Q_{u2}), \tag{1}$$

Where:

Q_{u1} = ultimate carrying capacity of raft on the homogenous soil composite,

Q_{u2} = ultimate carrying capacity of a single pile,

α = configuration factor (Table 5),

n_1 = number of piles.

The ultimate carrying capacity of raft on the homogeneous composite soil can be estimated as follows:

$$Q_{u1} = \left(BL - n_1 \frac{\pi D_1^2}{4}\right) q_{u1}. \tag{2}$$

q_{u1} can be determined by the general equation of Meyerhof (Das and Sivakugan, 2019), as follows:

$$q_{u1} = c_{comp}\overline{N}_c + q_1\overline{N}_q + \frac{1}{2}B\gamma_{comp}\overline{N}_\gamma \tag{3}$$

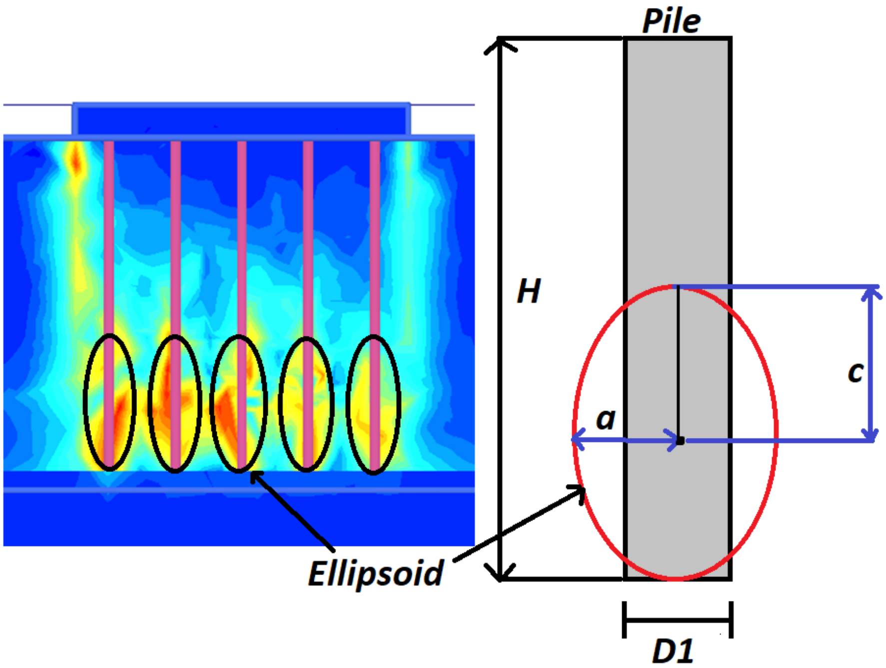

Fig. 18 Observed failure mechanism for piles in the combined foundation systém.

$$\overline{N}_c = N_c\left(1+\frac{B}{L}\frac{N_q}{N_c}\right)\left(1+0.4\frac{D_f}{B}\right)$$

$$\overline{N}_q = N_q\left(1+\frac{B}{L}\tan\varphi_{comp}\right)\cdot$$
$$\cdot\left[1+2\tan\varphi_{comp}\left(1-\sin\varphi_{comp}\right)^2\frac{D_f}{B}\right]$$

$$\overline{N}_\gamma = N_\gamma\left(1-0.4\frac{B}{L}\right)$$

$$N_c = \left(N_q-1\right)\cot\varphi_{comp}$$

$$N_q = \tan^2\left(\frac{\pi}{4}+\frac{\varphi_{comp}}{2}\right)\left(e^{\pi\tan\varphi_{comp}}\right)$$

$$N_\gamma = 2\left(N_q+1\right)\tan\varphi_{comp},$$

Where:
B = width of the raft,
L= length of the raft,
c_{comp} = cohesion of the homogenous soil composite (i.e., clay + stone column),
γ_{comp} = unit weight of the homogenous soil composite,
φ_{comp} = angle of shearing resistance of the homogenous soil composite,
n_1 = number of piles,
D_1 = diameter of the piles.

According to Etezad et al. (2015), the different soil parameters of the composite can be determined using Equations 4 to 8.

$$q_1 = \gamma_{comp}D_f$$

$$c_{comp} = A_s c_s + (1-A_s)c_c; \quad (4)$$

$$\gamma_{comp} = A_s\gamma_s + (1-A_s)\gamma_c, \quad (5)$$

Where:
D_f= depth of the raft,
A_s = replacement ratio (area of the stone columns over the area of the raft foundation),
A_{col} = column cross section,
c_s = cohesion of the stone columns,
c_c = cohesion of the soil (clay),
γ_s= unit weight of the stone column material,
γ_c = unit weight of the soil (clay);

$$\varphi_{comp} = \tan^{-1}[A_s\mu_s\tan\varphi_s + (1-A_s)\mu_c\tan\varphi_c]; \quad (6)$$

$$\mu_s = \frac{n}{1+(n-1)A_s}; \quad (7)$$

$$\mu_c = \frac{1}{1+(n-1)A_s}, \quad (8)$$

Where
φ_s= angle of shearing resistance of the stone column material,
φ_c= angle of shearing resistance of the clay soil,
n = stress ratio (between 2 and 6) (Mitchell and Katti, 1981).

The ultimate carrying capacity of a pile can be estimated by calculating the point bearing of the pile at the pile tip and the skin or frictional resistance of the pile (shaft). According to the failure mechanism of the combined foundation system observed in this study, the failure of the piles occurred by bearing and by shear in the soil near the piles' tip, which took an ellipsoidal shape (Fig. 18). The surface area of this shear failure plane was used to estimate the skin friction resistance of single pile.

Therefore, the ultimate carrying capacity of the piles (Q_{u2}) can be computed as:

$$Q_{u2} = \left[\frac{\pi D_1^2}{4}\left(q_2 N_q^* + c_2 N_c^*\right)\right] + c_u\left[2\pi a^2\left(1 + \frac{c}{ae} arc\,sin\,e\right)\right], \tag{9}$$

$$q_2 = \left(\gamma_{comp} \times H\right)\ or\ (0.5 p_a\, tan\,\varphi_2), \tag{10}$$

where
p_a = atmospheric pressure (100 kN/m²),
$c_u = c_c$= undrained shear strength of the clay,
$c_2 = 0, c_2$ = cohesion of soil supporting the piles,
φ_2 = angle of shearing resistance of the soil supporting the piles
N_q^* and $N_c^* = f(\varphi_2)$,
a and c = parameters $f(D_1)$,
$e^2 = 1 - \frac{a^2}{c^2}$.

The parameters a and c were deduced from the actual failure mechanism:

$$a = 3D_1$$

$$c = 7D_1;$$

Therefore,

$$Q_{u2} = \left[\frac{\pi D_1^2}{4}\left(q_2 N_q^*\right)\right] + c_u\left[2\pi a^2\left(1 + \frac{c}{ae} arc\,sin\,e\right)\right], \tag{11}$$

$$Q_{u2} = q_2\left[\frac{\pi D_1^2}{4} N_q^*\right] + c_u\left[2\pi a^2\left(1 + \frac{c}{ae} arc\,sin\,e\right)\right], \tag{12}$$

$$Q_{u2} = q_2 \overline{\overline{N}}_q + c_u \overline{\overline{N}}_c \tag{13}$$

Where:

$$\overline{\overline{N}}_q = \frac{\pi D_1^2}{4} N_q^*$$

$$\overline{\overline{N}}_c = \left[2\pi a^2\left(1 + \frac{c}{ae} arc\,sin\,e\right)\right].$$

By substituting the carrying capacity of raft on homogeneous soil composite soil (Q_{u1}) and carrying capacity of pile (Q_{u2}) in Equation 1, the ultimate carrying capacity of the combined foundation system can be expressed as

$$Q_u = \alpha\left[\left(BL - n_1\frac{\pi D_1^2}{4}\right)\left(c_{comp}\overline{N}_c + q_1\overline{N}_q + \frac{1}{2}B\gamma_{comp}\overline{N}_\gamma\right) + n_1\left(q_2\overline{\overline{N}}_q + c_u\overline{\overline{N}}_c\right)\right]. \tag{14}$$

To calibrate the analytical model, the results obtained by equation 14 were compared to the results of the present numerical analysis. An admissible discrepancy was noted between the different evaluated results. This divergence can be attributed to the assumptions considered in the derivation process of the analytical model. As a means of confining or narrowing the divergence between the different results, the parameter α was introduced in equation 14 and defined as the ratio between the results obtained by the numerical model and those computed from equation 14. The different values of this parameter are summarized in Table 5. By excluding the last three values of this parameter, an average value of $\alpha = 0.71$ was adopted for the present investigation, with a standard derivation of 0.03. Subsequently, the analytical model was validated against the results of the work reported by Sharma and Kumar (2021). As mentioned earlier, very few works in the literature have used combined stone columns and pile under a raft foundation. The comparison reveals that the analytical model slightly overestimates the carrying capacity of the combined foundation system by about 10.5 to 13.7 %). It is suggested that some physical modeling be conducted to calibrate the parameter α.

5. CONCLUSION

A numerical investigation was performed for combined stone columns and piles capped with rigid raft in soft clay using PLAXIS 3D. The following conclusions can been drawn from this investigation:

1. Combining stone columns and piles in one foundation system improves the carrying capacity of the system, modifies the soil foundation to a new upgraded composite ground, and certainly reduces the cost of the geotechnical work.
2. The ultimate carrying capacity of the combined foundation system increases with an increase in the number of piles in the system.
3. The carrying capacity of the combined foundation system improves with an increase in the diameter ratio of the piles and columns, angle of friction of the stone columns, modulus of elasticity of the clay soil, and a decrease in the length ratio L_c/L_p of the stone columns and piles.

Table 5 Calibration of the Developed Analytical Model for the Combined Foundation System (Eq. 14).

	Set No.	n_1	n_c	D_1 (m)	D_2 (m)	H (m)	S (m)	D_f (m)	B (m)	L (m)	Q_u (kN/m^2) Plaxis 3D	Q_u (kN/m^2) analytical model (Eq. 14)	α
Current study	8	4	21	0.6	1	20	4	2	20	20	243.1	356.03	0.68
	24	4	21	0.6	1	20	4	2	20	20	243.91	356.03	0.69
	25	4	21	0.6	1	20	4	2	20	20	252.72	356.03	0.71
	10	5	20	0.6	1	20	4	2	20	20	265.66	366.54	0.72
	22	5	20	0.6	1	20	4	2	20	20	251.45	366.54	0.69
	29	5	20	0.6	1	20	4	2	20	20	251.98	366.54	0.69
	30	5	20	0.6	1	20	4	2	20	20	258.52	366.54	0.71
	3	8	17	0.6	1	20	4	2	20	20	287.15	398.59	0.72
	9	8	17	0.6	1	20	4	2	20	20	274	398.59	0.69
	14	8	17	0.6	1	20	4	2	20	20	282.87	398.59	0.71
	26	8	17	0.6	1	20	4	2	20	20	272.75	398.59	0.68
	27	8	17	0.6	1	20	4	2	20	20	282.26	398.59	0.71
	11	9	16	0.6	1	20	4	2	20	20	293.55	409.44	0.72
	18	9	16	0.6	1	20	4	2	20	20	290.09	409.44	0.71
	23	9	16	0.6	1	20	4	2	20	20	289.7	409.44	0.71
	31	9	16	0.6	1	20	4	2	20	20	287.11	409.44	0.70
	32	9	16	0.6	1	20	4	2	20	20	286.95	409.44	0.70
	15	12	13	0.6	1	20	4	2	20	20	323.89	442.46	0.73
	16	12	13	0.6	1	20	4	2	20	20	307.99	442.46	0.70
	28	12	13	0.6	1	20	4	2	20	20	319.16	442.46	0.72
	19	13	12	0.6	1	20	4	2	20	20	321.46	453.63	0.71
	20	13	12	0.6	1	20	4	2	20	20	300.46	453.63	0.66
	33	13	12	0.6	1	20	4	2	20	20	329.58	453.63	0.73
	4	16	9	0.6	1	20	4	2	20	20	391.26	487.57	0.80
	17	16	9	0.6	1	20	4	2	20	20	352.92	487.57	0.72
	12	17	8	0.6	1	20	4	2	20	20	399.25	499.03	0.80
	21	17	8	0.6	1	20	4	2	20	20	339.95	499.03	0.68
	5	20	5	0.6	1	20	4	2	20	20	473.51	533.84	0.89
	13	21	4	0.6	1	20	4	2	20	20	515.25	545.58	0.94
	6	24	1	0.6	1	20	4	2	20	20	583.43	581.20	1.00
Sharma and Kumar (2021)	Piles with CSC 0.7mØ	4	5	0.5	0.7	6	1	1	4.8	4.8	284.29	317.71	–
	Piles with CSC 0.8mØ	4	5	0.5	0.8	6	1	1	4.8	4.8	299.48	347.05	–

4. Based on the optimization study, sets 28, 33, 4, and 12 were the chief leading sets (i.e., the sets having the highest improvement factor). These chief leading sets can increase the bearing capacity of the combined foundation system by almost 60–100%, compared with that of raft foundation resting on stone columns alone.
5. The combined foundation system fails by shear in the stone columns and soft soil and by bearing and shear failure of the piles' tip under the rigid raft. The failure of the foundation system starts slightly from the center of the raft and noticeably extends to its edges.
6. Due to presence of stone columns in the combined foundation system, the piles do not interact, and the stress transmitted by the piles to the soil does not overlap.
7. Equation 14, which was developed in this study, provides an analytical model for the prediction of the ultimate carrying capacity of the combined foundation system.

REFERENCES

Ahmed, D.: 2023, Geotechnical performance of combined stone columns/piles capped with reinforced concrete raft foundation in soft clay soil. Ph.D. thesis, Universiti Malaysia Sarawak.

Ahmed, D., bt Taib, S.N.L., Ayadat, T. and Hasan, A.: 2022, Numerical analysis of the carrying capacity of a piled raft foundation in soft clayey soils. Civ. Eng. J., 8, 4, 622–636. DOI: 10.28991/CEJ-2022-08-04-01

Ali, K., Shahu, J.T. and Sharma, K.G.: 2010, Behaviour of reinforced stone columns in soft soils.: An experimental study. Indian Geotechnical Conference, 620–628.

Ayadat, T.: 2022, Geotechnical performance of encapsulated and stabilized stone columns in a collapsible soil. Int. J. Geomech., 22, 6. DOI: 10.1061/(ASCE)GM.1943-5622.0002368

Ayadat, T. and Hanna, A.M.: 2005, Encapsulated stone columns as a soil improvement technique for collapsible soil. Proc. Inst. Civ. Eng.: Ground Improv., 9, 4, 137–147.

Chin, F.K.: 1972, The inverse slope as a prediction of ultimate bearing capacity of piles. Proceedings of the 3rd Southeast Asian Conference on Soil Engineering, Hong Kong, 83–91.

Das, A.K. and Deb, K.: 2014, Modeling of uniformly loaded circular raft resting on stone column-improved ground. Soils Found., 54, 6, 1212–1224. DOI: 10.1016/j.sandf.2014.11.014

Das, B.M. and Sivakugan, N.: 2019, Principles of foundation engineering (9th ed.). Cengage Learning.

El-Garhy, B., Abdel Galil, A., Youssef, A. and Abo Raia, M.: 2013, Behavior of raft on settlement reducing piles: Experimental model study. J. Rock Mech. Geotech. Eng., 5, 5, 389–399. DOI: 10.1016/j.jrmge.2013.07.005

Elias, V., Welsh, J, Warren, J. Lukas, R., Collin, J.G. and Berg, R.R.: 2006, Ground improvement methods. FHWA NHI-06-019 (Vol. 1) and FHWA NHI-06-020 (Vol. 2), 1056 pp.

Etezad, M., Hanna, A.M. and Ayadat, T.: 2015, Bearing capacity of group of stone columns in soft soil. Int. J. Geomech., 15, 2. DOI: 10.1061/(ASCE)GM.1943-5622.0000393

Ghazavi, M. and Afshar, J.N.: 2013, Bearing capacity of geosynthetic encased stone columns. Geotext. Geomembr., 10, 2, 47–53. DOI: 10.1016/J.GEOTEXMEM.2013.04.003

Han, J.: 2015, Principles and practice of ground improvement. John Wiley and Sons, 435 pp.

Hussin, J.D.: 2006, Methods of soft ground improvement. The foundation engineering handbook, 529–565.

Jenck, O., Dias, D. and Kastner, R.: 2005, Soft ground improvement by vertical rigid piles two-dimensional physical modelling and comparison with current design methods. Soils Found.,45, 6, 15–30. DOI: 10.3208/sandf.45.15

Lin, D. and Feng, Z.: 2006. A numerical study of piled raft foundations. J. Chin. Inst. Eng., 29, 6, 1091–1097. DOI: 10.1080/02533839.2006.9671208

Mali, S. and Singh, B.: 2020, 3D numerical modeling of large piled-raft foundation on clayey soils for different loadings and pile-raft configurations. Stud. Geotech. Mech., 42, 1, 1–17. DOI: 10.2478/sgem-2019-0026

Manojit, S. and Bhowmik, R.: 2017, 3D numerical analysis of piled raft foundation in stone column improved soft soil. Int. J. Geotech. Eng., 13, 5. DOI: 10.1080/19386362.2017.1368139

McCabe, B.A., McNeill, J. A. and Black, J.A.: 2007, Ground improvement using the vibro-stone column technique. Joint meeting of Engineers Ireland West Region and the Geotechnical Society of Ireland.

McCabe, B.A., Nimmons, G.J. and Egan, D.: 2009, A review of field performance of stone columns in soft soils. Proc. Inst. Civil Eng. – Geotech., 162, 6, 323–334. DOI: 10.1680/geng.2009.162.6.323

Mehrannia, N., Kalantary, F. and Ganjian, N.: 2018, Experimental study on soil improvement with stone columns and granular blankets. J. Cent. South Univ., 25, 4, 866–878. DOI: 10.1007/s11771-018-3790-z

Mishra, B.: 2016, A study on ground improvement techniques and its applications. Int. J. Innov. Res. Sci. Eng. Technol., 5, 1, 72–86. DOI: 10.15680/IJIRSET.2015.0501010

Mitchell, J.K. and Katti, R.K.: 1981, Soil improvement. Proc. Tenth Int. Conf. on Soil Mech. and Found. Eng., Stockholm, 4, 567-575.

Moseley, M.P. and Kirsch, K.: 2004, Ground improvement. CRC Press.

Naseer, S., Sarfraz Faiz, M., Iqbal, S. and Jamil, S.M.: 2019, Laboratory and numerical based analysis of floating sand columns in clayey soil. Int. J. Geo-Eng., 10, 1. DOI: 10.1186/s40703-019-0106-6

Nazari Afshar, J. and Ghazavi, M.: 2014, A simple analytical method for calculation of bearing capacity of stone-column. Int. J. Civ. Eng., 12, 1, 15-25.

Nehab, N., Baba, K., Ouadif, L. and Bahi, L.: 2018, Numerical simulations of ground improvement using stone columns in “Bouregreg Valley”. In: Bouassida, M. and M. Meguid, M. (eds.), GeoMEast 2017: Ground Improvement and Earth Structures, Sustainable Civil Infrastructures. DOI: 10.1007/978-3-319-63889-8_6

Remadna, A., Benmebarek, S. and Benmebarek, N.: 2020, Numerical analyses of the optimum length for stone column reinforced foundation. Int. J. Geosynth. Ground Eng., 6, 34. DOI: 10.1007/s40891-020-00218-x

Samangani, A.Y. and Naderi, R. : 2022, Numerical and large-scale laboratory study of rock column groups in sandy soil behavior improvement. Adv. Civ. Eng., 2022, 9259093. DOI: 10.1155/2022/9259093

Sexton, B.G., McCabe, B.A. and Castro, J.: 2014, Appraising stone column settlement prediction methods using finite element analyses. Acta Geotech., 9, 993–1011. DOI: 10.1007/s11440-013-0260-5

Sharma, S. and Kumar, S.J.: 2021, Behaviour of raft foundation supported by stone columns and combination with rigid piles in soft clay soils: 3D numerical study. Int. Res. J. Eng. Technol., 8, 9.

Singh, I. and Sahu, A.K.: 2019, A review on stone columns used for ground improvement of soft soil. Proc. 4th World Congress on Civil, Structural, and Environmental Engineering (CSEE’19), Rome. DOI: 10.11159/icgre19.132

Sinha, A. and Hanna, A.M.: 2016, 3D numerical model for piled raft foundation. Int. J. Geomech., 17, 2, 04016055. DOI: 10.1061/(ASCE)GM.1943-5622.0000674

Van Impe, W.F.: 1989, Soil improvement techniques and their evolution. Taylor and Francis, 125 pp.

Vu, A., Pham, D., Nguyen, T. and He, Y.: 2014, 3D finite element analysis on behaviour of piled raft foundations. Appl. Mech. Mater., 580–583, 3–8. DOI: 10.4028/www.scientific.net/amm.580-583.3

Xie, Y. and Chi, S.: 2020, Optimization method of reducing the differential settlements of piled raft foundations based on pile-to-pile interaction theory. Adv. Civil Eng., 2020, 1–14. DOI: 10.1155/2020/1521876

Appendix A Different configurations (or sets) of the combined foundation systém.

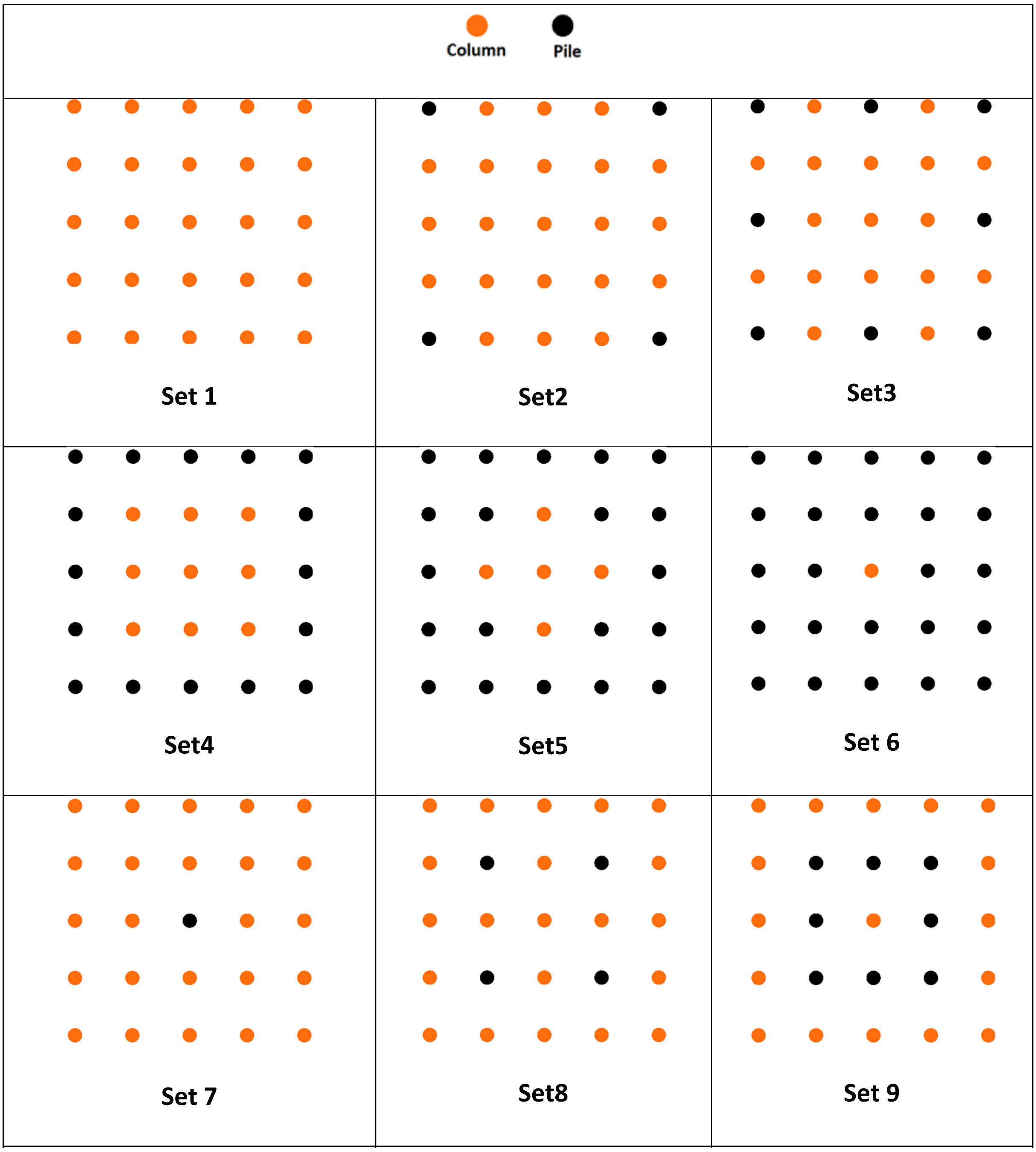

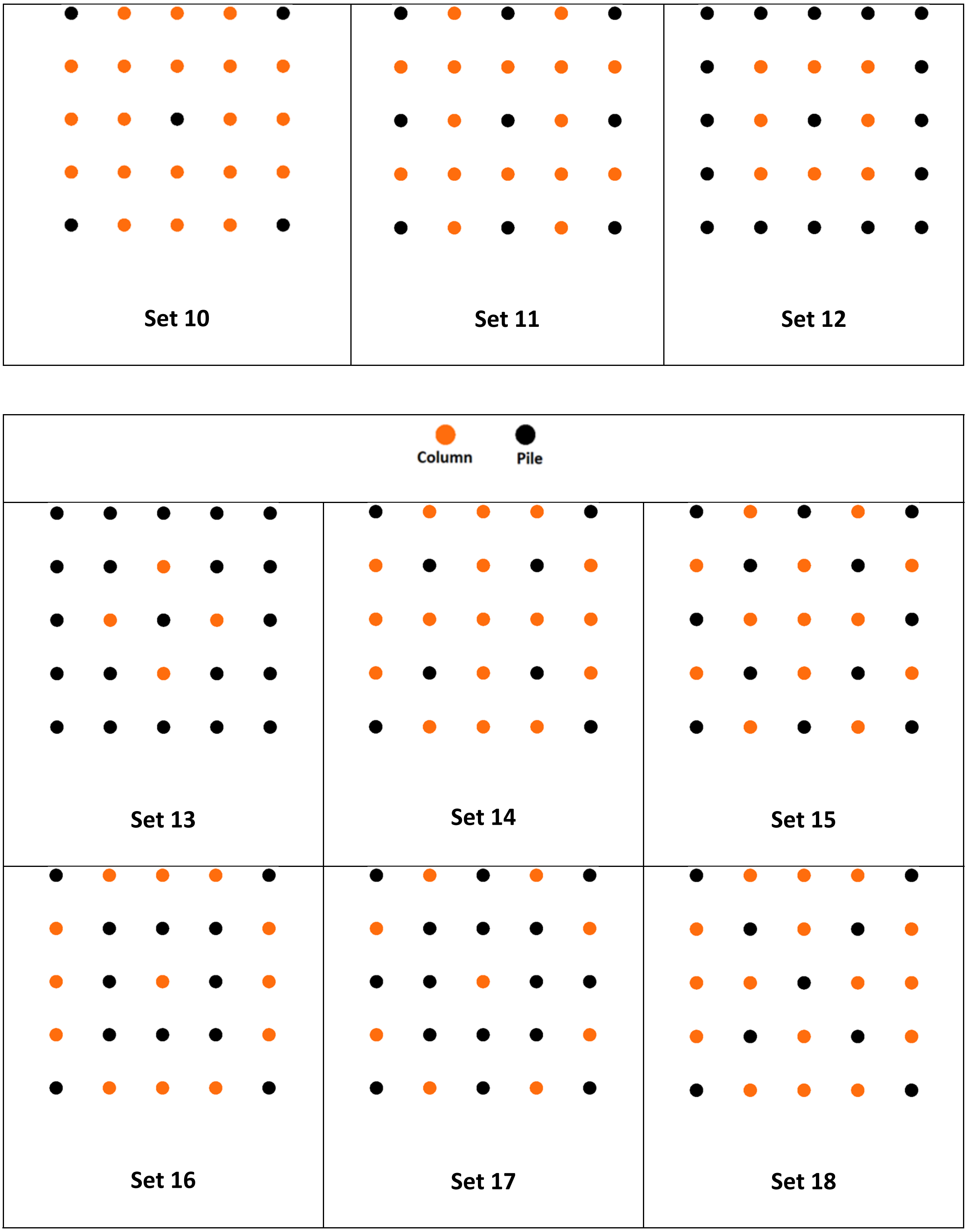
Set 10
Set 11
Set 12
Column
Pile
Set 13
Set 14
Set 15
Set 16
Set 17
Set 18

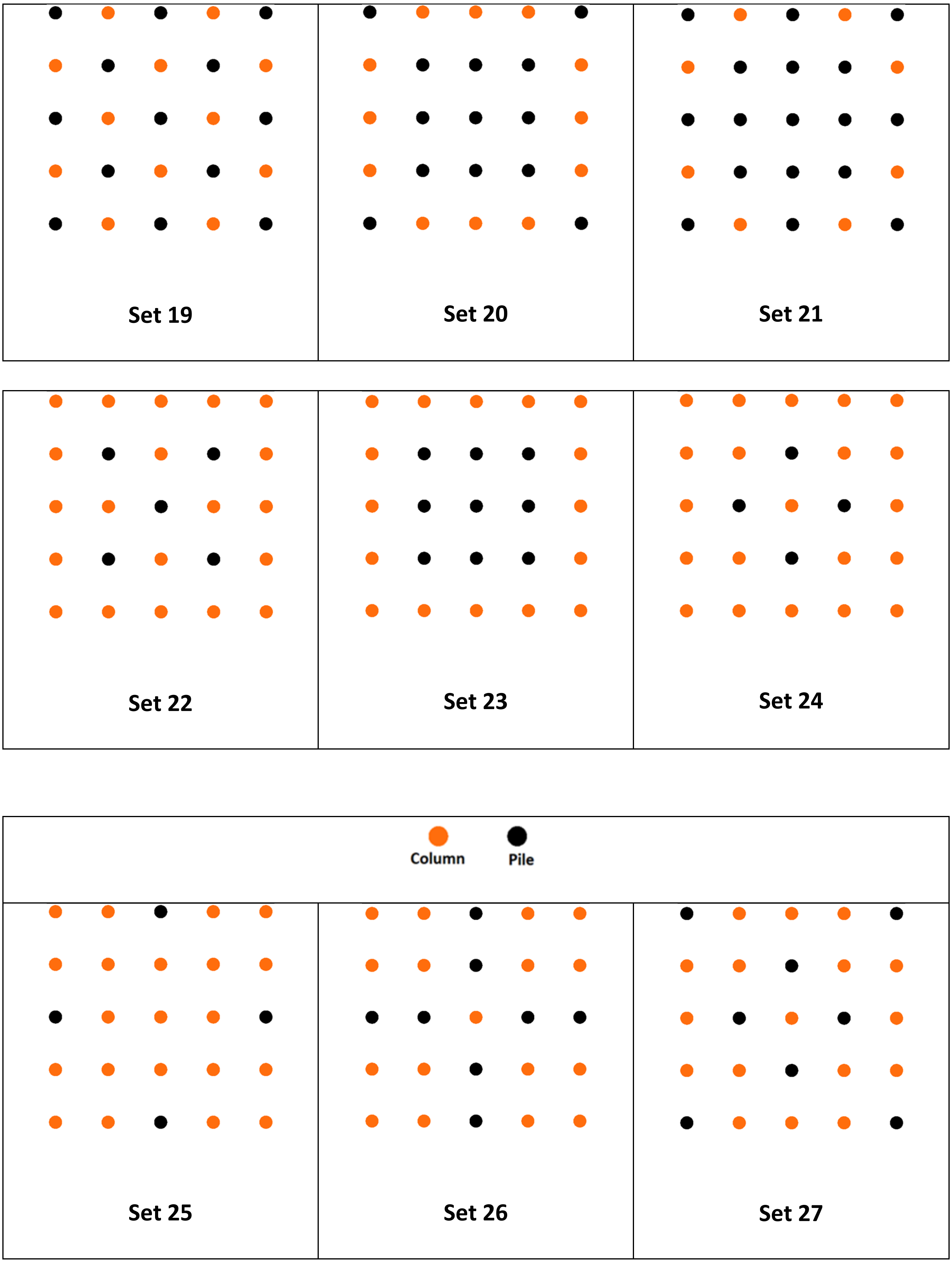
Set 19
Set 20
Set 21
Set 22
Set 23
Set 24
Column
Pile
Set 25
Set 26
Set 27

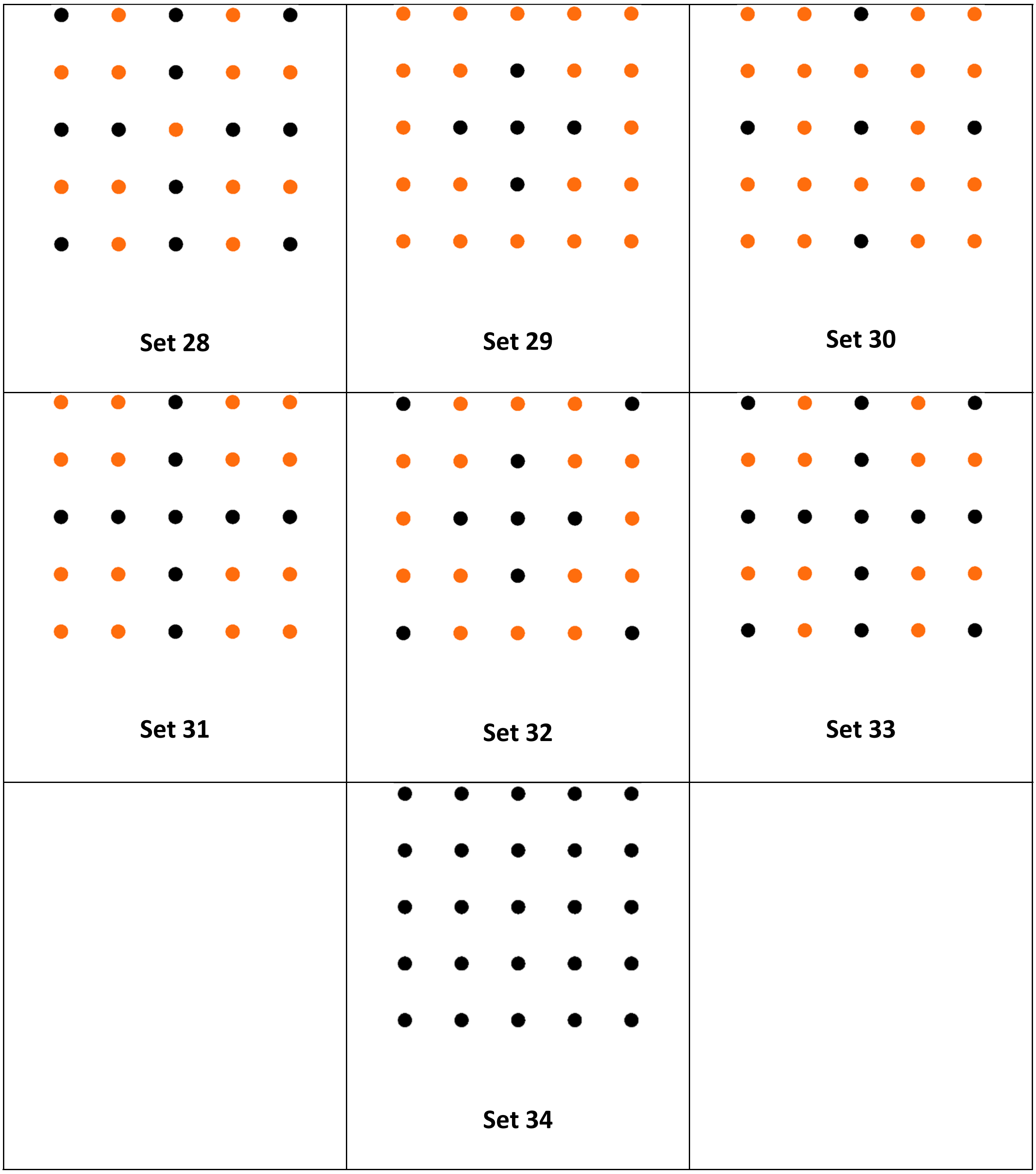
Set 28
Set 29
Set 30
Set 31
Set 32
Set 33
Set 34